

**EVALUATION OF GEOMAGNETICALLY INDUCED
CURRENTS EFFECTS ON POWER TRANSFORMERS**

BY
AYYOUB WAEL AL HOURANI

A Thesis Presented to the
DEANSHIP OF GRADUATE STUDIES

KING FAHD UNIVERSITY OF PETROLEUM & MINERALS

DHAHRAN, SAUDI ARABIA

In Partial Fulfillment of the
Requirements for the Degree of

MASTER OF SCIENCE

In

ELECTRICAL ENGINEERING

JANUARY 2018

KING FAHD UNIVERSITY OF PETROLEUM & MINERALS

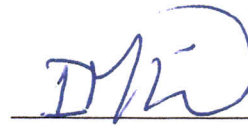
DHAHRAN- 31261, SAUDI ARABIA

DEANSHIP OF GRADUATE STUDIES

This thesis, written by **AYYOUB WAEL AL HOURANI** under the direction his thesis advisor and approved by his thesis committee, has been presented and accepted by the Dean of Graduate Studies, in partial fulfillment of the requirements for the degree of **MASTER OF SCIENCE IN ELECTRICAL ENGINEERING.**



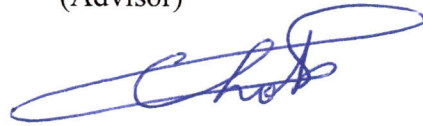
Dr. Ali A. Al-Shaikhi
Department Chairman



Dr. Ibrahim M. El-Amin
(Advisor)

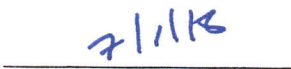


Dr. Salam A. Zummo
Dean of Graduate Studies

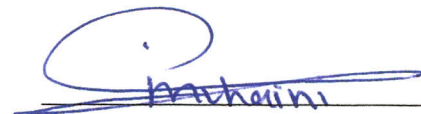


Dr. Chokri S. Belhaj
(Member)

7/1/16



Date



Dr. Mohammed M. Al-Muhaini
(Member)

© AYYOUB WAEL AL HOURANI

Jan. 2018

This Thesis is dedicated to

The soul of my AUNT EMAN

My Dear FATHER WAEL & MOTHER EMAN

My Wife MARAM

My Son GHAITH

ACKNOWLEDGMENTS

All praise and glory to Allah the most merciful, the most beneficent, who gave me the health, strength, and courage to complete my Master's degree.

I would like to express my deep appreciation to my advisor Prof. Ibrahim M. El-Amin for giving me the opportunity to become one of his students. I thank him for his efficient and constant support, help, motivation, and immense knowledge. His precious advice and thorough guidance played a critical role in completing this thesis.

I also would like to extend my appreciation to my dissertation committee members Dr. Chokri Belhaj and Dr. Mohammed Al-Muhaini for their insightful comments, support, and profitable questions which incited me to enhance my work.

I am very grateful to my company Saudi Power Transformers Company for its support and understanding during the study period.

I am thankful to the King Fahd University of Petroleum and Minerals (KFUPM) for providing me with the research facilities, precious resources and an environment conducive to intellectual growth for my master research.

TABLE OF CONTENTS

ACKNOWLEDGMENTS	V
TABLE OF CONTENTS	VI
LIST OF TABLES	VIII
LIST OF FIGURES	IX
LIST OF ABBREVIATIONS	XI
NOMENCLATURE	XII
ABSTRACT	XIV
ملخص الرسالة	XVI
1 INTRODUCTION	1
1.1 Overview	1
1.2 Thesis Motivations	3
1.3 Thesis Objectives	4
1.4 Thesis Contributions	5
1.5 Thesis Structure	6
2 LITERATURE REVIEW	7
2.1 Conducted Researches.	7
3 GEOMAGNETIC INDUCED CURRENT PHENOMENA	14
3.1 Basics of GMD and GIC Phenomena.	14
3.2 GIC Characteristics.	20
3.3 Effects of GIC on Power Transformers.....	22

3.3.1	GIC Impact on Magnetic Induction.....	22
3.3.2	GIC Impact on No-Load Current	25
3.3.3	GIC Impact on No-Load Loss and Core Temperature Rise.....	26
3.3.4	GIC Impact on Transformer Noise Level.....	27
3.3.5	GIC Impact of Reactive and Active Power Losses.....	28
3.3.6	GIC Impact on Winding Temperature Rise and Hot Spot Creation	30
3.4	Historical GIC Cases.....	32
4	PROBLEM FORMULATION AND METHODOLOGY	40
4.1	Problem Formulation	40
4.2	Magnetic Problem in FEMM.....	45
4.3	Transformer FEM Models.....	46
4.3.1	Model No.1 (Induction Model).....	46
4.3.2	Model No.2 (Stray Losses Model)	49
4.3.3	PSCAD Model.....	52
5	RESULTS AND DISCUSSIONS.....	54
5.1	Results	54
5.1.1	Model No.1 (Induction Model) Results	54
5.1.2	Model No.2 (Stray Losses Model) Results	65
5.1.3	Model No.3 (PSCAD Model) Results.....	72
5.2	New Transformer Design.	77
5.3	Cost-benefit Analysis	85
6	CONCLUSIONS AND FUTURE WORK	90
6.1	Conclusions	90
6.2	Recommendations for Future Work.....	92
	REFERENCES.....	93
	VITAE	97

LIST OF TABLES

Table 3.1, Thermal time constant for main materials	31
Table 3.2, Main Reported Transformers Damage / Over-Heating Contributed to GIC ...	32
Table 3.3, Main GIC reported cases from 1989 to 2015.	39
Table 4.1, 60 MVA, 132/13.8 kV transformer main windings parameters.	43
Table 4.2, 60 MVA, 132/13.8 kV transformer main core parameters.	44
Table 5.1, Obtained flux density shift for different GIC levels, Case 1	57
Table 5.2, Core loss and noise level increase for different GIC levels.....	59
Table 5.3, Obtained flux density shift for different GIC levels, Case 2	61
Table 5.4, Core loss and noise level increase for different GIC levels.....	62
Table 5.5, Obtained flux density shift for different GIC levels, Case 5.	63
Table 5.6, Transformer main parameters with different volt per turn values.	64
Table 5.7, Transformer windings losses at different GIC levels, Case No.1.....	66
Table 5.8, Transformer windings losses at different GIC levels, for Case No.2.	68
Table 5.9, Winding temperature rise during different GIC level.....	69
Table 5.10, Core materials characteristics.	77
Table 5.11, Core materials costing rate, as of Q4-2017.....	78
Table 5.12, Transformer windings losses at different GIC levels	82
Table 5.13, Winding temperature rise in improved Case No.1	82
Table 5.14, Summarized cost-benefits analysis of new transformer design.....	88
Table 5.15, Percentage increase of new design cost.	89

LIST OF FIGURES

Figure 3.1, Flow of GIC in a power network.....	15
Figure 3.2, GIC flow through grounded neutral connections of power transformers.....	16
Figure 3.3, Flux density shift caused by DC current	17
Figure 3.4, Effect of DC, Part-cycle (Half-cycle) saturation of transformer core	18
Figure 3.5, GIC profile at the Ottawa in Canada during the GMD 1989.	21
Figure 3.6, Permeability of core in function of BH curve.	24
Figure 3.7, Leakage field components on winding conductor.....	29
Figure 3.8, Principal mechanisms of GMD coupling with high voltage network	34
Figure 3.9, Magnetic density in nT across North America during GMD in 1991	35
Figure 4.1, Model No.1 (Induction Model).	47
Figure 4.2, Magnetization Curve of M080-23P5-DR core grade (BH Curve)	48
Figure 4.3, Model No.2 (Stray Losses Model).	50
Figure 4.4, Flow Chart of Model No.1 and Model No.2.	51
Figure 4.5, Model No.3 (PSCAD Model).....	52
Figure 5.1, The defined BH curve in FEMM based on actual data	54
Figure 5.2, Defined core characteristics in FEMM tool.	55
Figure 5.3, FEM induction model, normal condition with zero GIC current.	56
Figure 5.4, New operating flux density for different GIC levels.....	58
Figure 5.5, Core temperature rises at different GIC levels.	60
Figure 5.6, Three cases resulted flux density at different GIC level.	64
Figure 5.7, Leakage magnetic flux density in Case 1 with 100 A GIC.	67
Figure 5.8, Leakage flux in Case 2 with 100 A GIC.	69

Figure 5.9, Main transformer parameters defined in PSCAD.	73
Figure 5.10, Defined saturation curve parameters in PSCAD.	73
Figure 5.11, Magnetization current waveform with zero GIC current.	74
Figure 5.12, Magnetization current waveform with 50 A GIC current.	75
Figure 5.13, Magnetization current waveform with 100 A GIC current.	75
Figure 5.14, A linear relationship between GIC and reactive power consumption.	76
Figure 5.15, Flow chart of the adopting mechanism of new design techniques.	84

LIST OF ABBREVIATIONS

GMD	:	Geomagnetic Disturbance
GIC	:	Geomagnetically Induced Current
FEM	:	Finite Element Method
FEA	:	Finite Element Analysis
CME	:	Coronal Mass Ejections
UHV	:	Ultra-High Voltage
EHV	:	Extra-High Voltage
MMF	:	Magnetomotive Force
HiB	:	High Induction grain oriented
CGO	:	Conventional Grain Oriented
ERC	:	Earth Return Currents
UMEC	:	Unified Magnetic Equivalent Circuit
HVW	:	High Voltage Winding
LVW	:	Low Voltage Winding

NOMENCLATURE

B	:	Magnetic field density
H	:	Magnetic field intensity
I_{gic}	:	GIC current
v/t	:	Volt per turn value
A_c	:	Core cross section area
f	:	Frequency
ϕ_{dc}	:	DC flux shift
N	:	Number of HV winding turns
\mathcal{R}	:	Reluctance
VA/kg	:	Volt ampere per Kg fore built core
I_m	:	Magnetization current
w	:	Watts/kg for a particular operating peak flux density
K_p	:	Core building factor
W_t	:	Core total weight
K_c	:	Factor representing extra loss occurring at the corner joints
t	:	Thickness
k_1	:	Constant depends on material
k_2	:	Constant depends on material
B_{rms}	:	Effective flux density
B_{mp}	:	Peak flux density
n	:	Steinmetz constant
ω	:	Angular frequency
B_x	:	Radial component of magnetic flux density

B_y	:	Axial component of magnetic flux density
μ	:	Magnetic permeability
ρ	:	Resistivity
S	:	Complex power
Q	:	Reactive power
P	:	Active power
X	:	Leakage reactance

ABSTRACT

Full Name : [Ayyoub Wael Abel Muniem Al Hourani]
Thesis Title : [Evaluation of Geomagnetically Induced Currents Effects on Power Transformers]
Major Field : [Electrical Engineering]
Date of Degree : [January 2018]

Power transformers are one of the major components in power system that might be negatively affected by Geomagnetically Disturbances (GMD). During the magnetic storm, the magnetic field of the earth might be disturbed, thus generating induced voltages that might create undesired currents into power network. This thesis attempts to address the major effects of those induced Geomagnetically Induced Currents (GIC) on power transformers through addressing the part-cycle saturation and its impact on core losses, core noise, core temperature rise and reactive power absorption. Additional stray losses generated in windings and transformers structural parts due to the part-cycle saturation are investigated in this thesis using Finite Element Method (FEM) tool, FEMM.

This thesis aims to support power transformers designers with a comprehensive study of major effects of GIC phenomena on power transformers, and provide designers with a certain power transformers design techniques to investigate the major effects of a certain GIC level that transformers must survive against it. An actual power transformer parameters of 60 MVA, 132/13.8 kV have been used in all of conducted simulations. A Finite Element Method (FEMM) tool and PSCAD software are utilized in this evaluation.

A certain modifications on existing 60 MVA power transformer have been proposed to improve the withstand ability level against GIC event. Such as redesigning the top and

bottom parts of windings, utilizing upgraded low loss core material, enhance the cooling mechanism of core and designing a transformer with the lower number of turns to reduce the Magnetomotive Force (MMF) during GIC event. A cost-benefit study has been also conducted to find out the cost impact of generating transformer that can survive against the certain level of GIC currents.

ملخص الرسالة

الاسم الكامل: أيوب وائل عبد المنعم الحوراني

عنوان الرسالة: تقييم تأثير التيارات الجيومغناطيسية على عمل محولات الطاقة الكهربائية

التخصص: الهندسة الكهربائية

تاريخ الدرجة العلمية: كانون الثاني 2018م – ربيع الأول 1439هـ

تمثل المحولات الكهربائية أحد أهم عناصر الشبكة الكهربائية، وتعتبر من أكثر مكونات الشبكة الكهربائية عمراً، وهي من العناصر ذات الوثوق المرتفع جداً. خلال فترة خدمة المحولات بالشبكة الكهربائية قد تتعرض لعدة ظروف غير عادية قد تسبب اعطالاً لها إن لم تكن هذه المحولات مصممة لتحملها. واحد من هذه الحالات التي قد تتعرض لها محولات الطاقة الكهربائية هي التيارات الجيومغناطيسية المولدة بسبب الإضرابات الجيومغناطيسية المنبعثة من الشمس خلال فترة ذروة نشاطها. هذه التيارات الجيومغناطيسية تؤثر بشكل سلبي على أداء المحولات من خلال قيادة المحول للعمل في مراحل الإشباع للقلب الحديدي، مما قد يزيد من سحب التيار الكهربائي الممغنط، مما قد يؤثر على ارتفاع درجات الحرارة لتتجاوز الحد المسموح به وبالنهاية قد تفقد المحول من الخدمة.

هدف هذه الدراسة هو كشف وتحديد جميع الأجزاء المتأثرة في المحولات الكهربائية بالتيارات الجيومغناطيسية، بالإضافة إلى طرح الحلول لزيادة قدرة المحولات الكهربائية على تحمل مثل هذه الظروف. قامت هذه الدراسة على الاستناد إلى تقاضيل محمول حقيقي موجود في الخدمة حالياً في المملكة العربية السعودية، وهو 60 ميغا فولت أمبير بفولتية قدرها 13.8/132 كيلو فولت. بالإضافة إلى دراسة تأثير جميع الحلول المطروحة على سعر المحول واختيار الأنسب حسب الظروف التي سيخدم بها المحول. كما تم عمل عدة نماذج للمحول باستخدام برامج (FEMM) القائمة على مبدأ الأجزاء المحددة لمحاكاة سلوك المحول ومحاكاة كمية المجال المغناطيسي المفقود. وقد تم استخدام برنامج (PSCAD) لدراسة العلاقة ما بين التيارات الجيومغناطيسية وكمية الطاقة المسحوبة من المحول.

CHAPTER 1

INTRODUCTION

1.1 Overview

Fluctuations of solar radiation stream passing the earth's atmosphere, which has a peak every 11 years, might affect the earth's magnetic field, and thus Geomagnetically Induced Currents (GIC) appear in the power network. The main characteristics of these currents are considered as very low frequency currents, thus viewed as Direct Currents (DC), which might cause malfunctions in power network and lead to regional blackout, which can also incur large costs and risk to society. A Geomagnetic Disturbance (GMD) can last few days and continually generates the low frequency GIC currents. The common signature of the GIC current is Low to moderate magnitudes of GIC current last for several hours, interrupted by short-duration with high-peak pulses.

The sun has solar activities that occur all the time, but every 11 years on an average these activities peak occur. Geomagnetic Disturbance (GMD) might negatively affect the operation of the electric power systems that are located in high geomagnetic latitude zones. The most severe reported GMD events due to peak solar activities were in March 1989, in that event the Hydro Quebec high voltage transmission network in Canada experienced blackout. Investigations have shown that the failed transformers saturated due to flow Geomagnetically Induced Current (GIC).

This event had open researchers' eyes to the importance of investigation of such a phenomena to evaluate and assess the effects of GMD and GIC on major high voltage network components, specifically the power transformers.

Power transformers lifespan is comparatively very long. On an average, it is between 25 to 30 years. During such a long life period, the transformer quality index should be very high to survive not only under normal operating conditions but also to several abnormal conditions. Taking into account all expected abnormal conditions during the design stages of power transformers will definitely help to withstand such severe conditions.

The flow of GIC current through power transformers can cause part-cycle saturation. Which will increase reactive power absorption, current harmonic generation, system voltage instability, transformer overheating and eventually failure and breakdown of transformers. Therefore, an accurate assessment of the GIC and its effect on power system during a given GMD is very important.

There have been many reported significant GMD events that forced the transformers to be taken out of service for some weeks, and in some cases caused a blackout for a few hours in Canada in 1989, in South Africa 2003 and 2004 and in Sweden in 2003.

Since 1989, after the Hydro Quebec system collapse, certain GIC levels constraints started appearing in many transformers specifications. Those constraints of GIC currents have been specified based on detailed study of geomagnetic locations, high voltage power system parameters and earth conductivity. Power transformers manufacturers have to prove the capabilities of their transformers to those GIC levels.

1.2 Thesis Motivations

Based on the survey conducted on several power transformers manufacturers (in Europe and Canada), the lack of understanding of GIC phenomena and its impact on transformers have been figured out. In addition to that, no specific design techniques are followed in many power transformers manufacturers to overcome the GIC effect on power transformers. This thesis comes to fill this gap and gives some certain accurate techniques to evaluate the GIC effects and improve transformer design to survive when GIC phenomena occur. The cost-benefits study of the improved transformer design is conducted at the end of this thesis to help entities to decide to invest more in power transformers to obtain stronger transformers against GMD.

1.3 Thesis Objectives

This thesis comes to support power transformers designers with a comprehensive study of major effects of GIC phenomena on power transformers, and provide designers with a certain power transformers design techniques to investigate the major effects of a certain GIC level that transformers must survive against it. The main thesis objectives are summarized as follows:

1. To conduct a detailed literature review on GIC. The purpose is to have a clear understanding of GIC phenomena and identify the impact of GIC on power transformers.
2. To evaluate the impact of GIC on the selected power transformer. A Finite Element Method (FEM) tool and PSCAD software are utilized in this evaluation.
3. To propose power transformer design techniques taking into account the GIC phenomena into consideration, to improve power transformers withstand ability level against GIC phenomena.
4. To evaluate cost-benefits of the proposed design techniques.

1.4 Thesis Contributions

The main thesis contributions can be summarized in the followings points:

1. Modeling power transformers using Finite Elements Method (FEM) during the GIC phenomena. Two detailed FEM models have been created to simulate the power transformer behavior when subjected to such a phenomena. The first model is to find out the exact excessive induction of transformer core, and the second model is to evaluate the additional stray losses that might occur.
2. Modeling of power transformer response to the GIC phenomena using a PSCAD tool. The saturation behavior of power transformer has been modeled using the PSCAD to find out the relationship between GIC levels and absorb reactive power.
3. Evaluate the eddy current losses in windings using FEMM tool, by finding out the exact leakage flux components (axial and radial) and to control it by redesigning the winding parts where the radial leakage flux densities are dominant.
4. Specify the main locations in power transformer where magnetic shunts should be added in parallel with steel structure parts to avoid any hotspot creation (Tank Wall, Core Clamps), Based on FEM analysis of magnetic leakage flux distribution.
5. Propose design techniques that reduce the effects of GIC level on power transformers with their cost-benefits analysis, such that core design, windings design, utilizing non-magnetic materials in tank structure.

1.5 Thesis Structure

Besides the introduction, the thesis is organized as follows: Chapter 2 gives a literature review on conducted researches related to GIC phenomena and its impact on power transformers. Chapter 3 studies the GIC characteristics and its effects on power transformers. Chapter 4 states the problem formulation and methodology. Chapter 5 discusses the three models of power transformer to evaluate and investigate the effects of GIC on power transformers (two FEM models and one PSCAD simulation), in addition to discussing the proposed improved design techniques with cost-benefits analysis. Chapter 6 presents the main conclusion points and the scope of a proposed recommendation regarding future work.

CHAPTER 2

LITERATURE REVIEW

This chapter presents a review of the literature published related to GIC impacts on power transformers.

2.1 Conducted Researches.

Many researchers addressed the GIC phenomena over the last 30 years. The main GIC effects on power transformers have been studied using a mathematical model, that explicitly incorporating the electric and magnetic circuits in [2]. Many transformers types connected to National Grid in England and Wales have been used in this study to predict the main GIC effects. The proposed model has been validated by conducting DC injection tests on various types of transformers. Finite Element Method (FEM) techniques have been also utilized to find out the losses and increased temperature rises of different transformer components.

The increase in tank losses due to increase in the leakage flux entering into the transformer tank wall caused by GIC current have been investigated using 2-D FEM analysis in [7]. The main factors that affect the tank loss increase with GIC have been determined for different transformer types. Furthermore, the impact of installing the tank wall shunt on the inner surface on tank losses increase has been also investigated in [7].

The main impacts of GIC phenomena on power transformers, capacitive components and relays in power system network have been qualitatively and quantitatively studied in [4]. The main cases of transformers failure or overheating reported in North America and around the world, caused by GIC have been shortlisted and explained in [4].

The main impact on the growing of GIC has been studied in [9]. These include the conductor's resistances and structures, transmission lines length, type of transformers, substation grounding resistance and the network topology. The behavior of a specific power transformer design and rating under different GIC current levels with different loading conditions, in the presence of non-magnetic stainless steel, to limit local overheating, have been simulated using 3-D FEM analysis in [9], to find out the maximum GIC current levels the transformer can withstand without damage.

In addition to neutral blocking devices, many mitigation techniques have been proposed in the literature. A mitigation technique that consists of connecting switching devices at transformer neutral grounding connection point have been proposed to reduce the effects of GIC on power system [27]. Another mitigation technique that eliminates the detrimental effects of Earth Return Currents (ERC) of HVDC transmission is proposed in [28]. This technique is called the potential compensation method, in brief by balancing the network DC voltage by adjusting the DC voltage equilibrium of AC power systems.

The behavior of three-phase power transformers with various core constructions in the presence of GIC has been investigated in [11]. In addition, the main significant parameters that can affect the reactive power consumption during GIC event have been highlighted. The paper concluded that for accurate power system study dealing with the GIC, the transformer dynamics should be considered.

To determine the main effect of DC offset on power loss and excitation current of the iron core, a measurement system for grain-oriented electrical steel single sheet sample has been conducted, a sinusoidal magnetic flux density with superimposed DC component have been applied on single sheet tester with certain levels. The results showed large addition in power losses and large increases to the magnetizing current as per [26].

As the transformers inductance values change from un-saturated values to saturated ones every cycle, the growth of GIC function of transformers effective inductances have been illustrated in [10]. The transformer inductance can limit the high GIC variations produced by the high electric fields. This paper studied the interaction between transformers and GIC.

The semi-cycle saturation effect resulting from the DC-biased excitation of the magnetic core has been explained in [6]. This phenomena has been numerically modeled and applied to different transformer designs. The no-load and different on-load conditions analysis have been performed and addressed in [6].

A methodology to investigate both the effect of GIC on power transformer as a function of GIC magnitude, and the transformer designs withstand ability for a wide range of magnitude and duration of GIC pulses have been proposed in [3]. It includes the calculation of magnetizing current with associated VAR swings and harmonics. This is to find out the increase in core loss, core noise and load losses.

The acceptable DC current limit to the certain construction of power transformer with the resulted temperature rises of different transformer components have been investigated in [24] using FEM simulation and analytical studies.

The harmonics content of excitation current and reactive power consumption of power transformer with DC biased caused by GIC or HVDC transmission system in monopole grounding return mode have been analyzed in [25] based on piecewise iron core model.

There have been many reported significant GMD events that forced the transformers to be taken out of service for some weeks, and in some cases caused a blackout for a few hours in Canada in 1989, in South Africa 2003 and 2004 and in Sweden in 2003 [4].

High voltage networks are more affected by geomagnetic storm than lower voltage system. Thus an accurate modeling of the interaction between the high voltage power system (EHV and UHV) and a specific severity level of GMD has been presented in [13]. In March 1989, in Quebec province of Canada, more than 6 million people had blackout for about 9 hours in addition to the possibility of damaging large power transformers.

The model focus on the time and spatial changes of geomagnetic fields during a storm in order to evaluate the GIC currents that will flow in power system network. The model has utilized the collected data in North America over 20 years. As a result, a computer model that determines the variation in B-field has been created. The second approach in [13] was to create a model for earth conductivity, to specifically determine the changes in induced earth surface electric fields. Then the electric networks have been also modeled to find out the exact generated GIC currents values. So in [13] three models have been created, the first is to simulate the magnetic field density, the second is to simulate the earth parameters and the induced electric fields and the third to find out the GIC value. The complete model has been validated by comparing its results with observed GIC values in past.

One of the main projects in GIC assessments is the one conducted on the Swiss network in [14]. A specific GMD cases of the Swiss transmission network have been studied and numerically evaluated based on reported GMD events in the past. The conclusion of this study stated that the overall risk level occurred by geomagnetic disturbances in Swiss network is relatively low as the Swiss network can survive against those low GIC levels.

In Switzerland, a geomagnetic storm can generate about 0.2 V/m, and in the worst case not more than 0.5 V/m, wherein Scandinavian counties the voltage per kilometer range is from 1 to 7 V/m that can be observed. That is why the GIC effects in Switzerland would not be that significant. However, the whole Switzerland electric system parameters have been modeled for the exact evaluation of the impact of GIC current that might be induced in the worst case, which is 11 A in 380 kV network. The study has also considered the 1 V/km, which is not realistic in Switzerland networks. It found that the GIC currents would be still not exceeding 20 A. Which is acceptable to Swiss transmission network.

On the basis of reported GIC cases in Chinese electric network of 500 kV, and the calculated GIC values for 750 kV, an estimation of GMD risk on the future Chinese UHV network 1000 kV has been highlighted in [15]. The purpose of this study is to overcome all the issues related to the expected high GIC current that might flow in the upgraded UHV network. UHV network has much lower DC resistance, DC resistance for 1000 kV UHV is lower than of 500 kV. The risk assessment has been made for 1000 kV based on historical data and estimated new network model.

The GIC impact is usually most severe in the areas closer to the earth poles rather than the central ones, but based on the historical records, no place in Europe is 100% safe

from such solar storm phenomena. The Austrian power grid has been modeled to evaluate the effects of such a phenomena on its network in [16]. Austria is located in central of Europe, where it is considered mid-latitude region for GMD. The model has made based of the same conditions recorded in March 2015. The peak GIC found 10 A, which is low value due to DC resistance of Austria network.

The GIC impact on 400 kV power system in Finland has been conducted in [17]. Finland is located in a zone where a GIC is frequently generated due to solar storms. A continuous GIC monitoring system was installed on 400 kV network to monitor and record all the GMD events. Finland had experience of 200 A for 1 minute on March 24th, 1991, without reported equipment failure or major malfunctioning. Finland is applying a special test of DC magnetization on all transformers at sites to record the network behavior and take the safe operation precaution. The detailed DC procedure and measured values are represented in [17].

To improve the modeling of geomagnetically induced current, the substation grounding resistance is removed and an alternative algorithm is provided in [35] to estimate the resistances from the GIC measurements. An analytical technique is developed in this paper which derives the substation grounding resistance from the GIC measurements. In [36], a model relates the GIC current with its deriving electric field is proposed and validated based on actual collected data from American Transmission Company.

A spatial model of the power grid with the ring configuration that allows considering a geographical arrangement of the power transformers in the geomagnetically induced current calculation is presented in [37]. It concludes that ring configuration of power grid causes the highest impact on power transformers.

All of the above studies have considered the no-load operation condition. In this thesis, the no-load and different loaded conditions will be studied during GIC event. The approach of finding out an accurate magnetic density shift in this thesis is by using FEM analysis, wherein other researches no clear approaches have been stated. The detailed losses during GIC event will be evaluated in this thesis. In contrast, others have focused on no-load and resistive load losses only, two of them have studied the stray losses in structural parts.

Furthermore, none of the above researchers have proposed new design techniques to survive against certain GIC level. In this thesis, a comprehensive study of the effects of GIC on power transformers will be taken place, and improved transformer design techniques using FEM tool will be investigated to overcome the GIC phenomena.

CHAPTER 3

GEOMAGNETIC INDUCED CURRENT

PHENOMENA

This chapter addresses the basics of GIC phenomena and the major affected parts in power transformers during the GIC event. It will also present the main reported GIC events worldwide since 1989.

3.1 Basics of GMD and GIC Phenomena.

Strong and complex magnetic fields are produced due to various events that occur on the surface of the sun. Sun activities and the ejection of plasma, due to coronal mass ejections (CME) and high speed solar wind streams, and its interaction with the earth's magnetic field can cause a disturbance of the magnetic field of the earth. This naturally occurring phenomenon in the earth's magnetic field called a Geomagnetic Disturbance (GMD).

The changing magnetic field induces currents/voltages in the loops formed by transmission lines, grounded-wye transformers, that are the entry points, and the paths through the earth between the transformer neutrals. The earth surface potential (geoelectric field) can also be changed, resulting in the flow of Geomagnetically Induced Current (GIC) as shown in Figure 3.1.

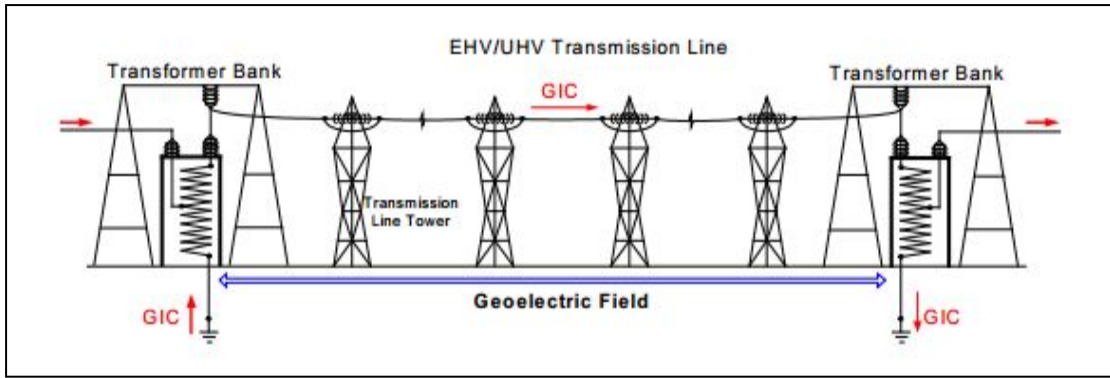


Figure 3.1, Flow of GIC in a power network.

GIC is quasi-dc current because of its generally low frequency, typically 0.01 Hz to 0.5 Hz. A GMD event might last few days, and continually generates varying levels of GIC (low to moderate). The GIC risk is not uniform across the power system. It depends highly on the actual characteristics of the GMD event and each part of the power system. The main factors that play critical roles in determining the risk exposures to power transformers are: Geographical region, local soil resistivity, coastal effect, network topology, design and technical specification of the power transformer, storm duration, storm intensity, loading and many others [1].

The flow of GIC current can cause part-cycle saturation in power transformers that can increase reactive power absorption, current harmonic generation, system voltage instability, transformer heating and eventually failure and breakdown of transformers. Therefore, an accurate assessment of the GIC and its effect on power system during a given GMD is very important. The GIC flow through the transformer is described in Figure 3.2.

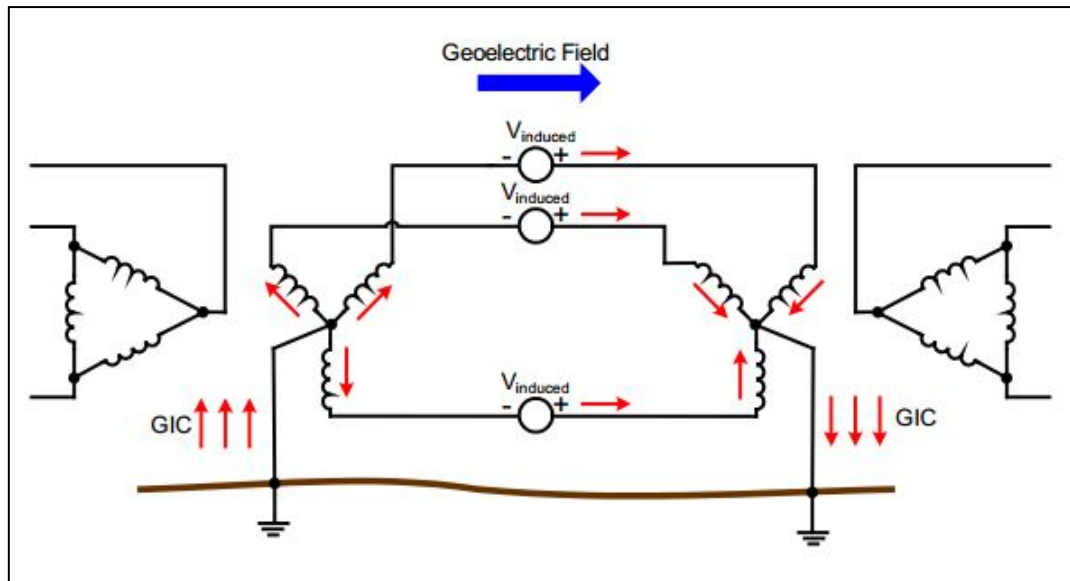


Figure 3.2, GIC flow through grounded neutral connections of power transformers.

When the induced voltage, $V_{induced}$, appears in the power system, almost all of this voltage appears initially across the unsaturated transformers magnetizing inductances. This is because transformers inductances are much greater than those of the transmission lines. The induced voltage has a very low frequency (quasi-dc). It causes an increase in the DC flux density offset, allowing only a small amount of DC current to flow. This continues till the transformer core flux density reaches the saturation level.

The magnitude of magnetic flux density shift from the normal operating point depending on the magnitude of the injected DC current, number of turns of HV winding, and the magnitude of equivalent reluctance to DC flux path. As a result, the DC flux will add to the amplitude of the flux (AC one) in one-half cycle and subtract from the amplitude of the flux in the second half cycle as shown in Figure 3.3.

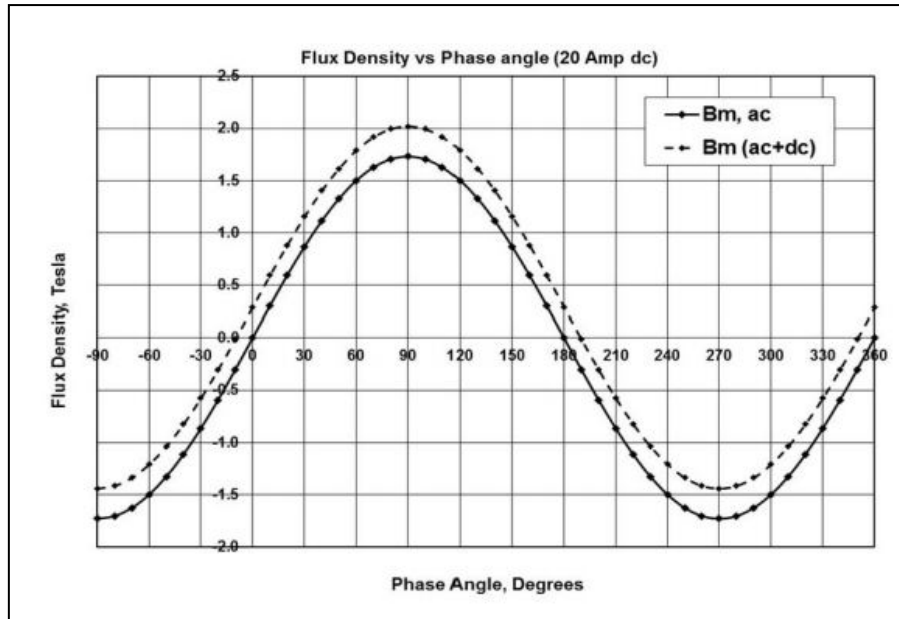


Figure 3.3, Flux density shift caused by DC current [1].

When the DC flux is large enough, the peak combined flux density (AC+DC) in the core across the linear region and the knee point in one half of the cycle result in core saturation for a small part of a cycle. This is referred to as part-cycle saturation. Figure 3.4 shows the (B-I) magnetic flux density-current characteristics. It represents the B-H curve of magnetic core material since magnetic field strength (H) is proportional to current. The B-H curve characteristics of the transformers core materials are nonlinear. Higher reluctance will be provided by core for higher magnitudes of DC and therefore results in a smaller incremental in the flux density shift and a higher peak magnetizing current pulse.

Three-leg cores construction transformers provide a high reluctance path to additional DC flux. The high reluctance path of DC flux from the top yoke to the tank top cover, to the transformer tank walls, then return to the core bottom yoke through also high reluctance path from the transformer tank bottom. This core type is less susceptible to part-cycle core saturation. However, it is susceptible to high magnitudes of magnetizing

current. Single-phase, shell form, and five-leg core form transformers present lower reluctance to the DC flux within the core. They are more susceptible to part-cycle core saturation at lower levels of DC [1].

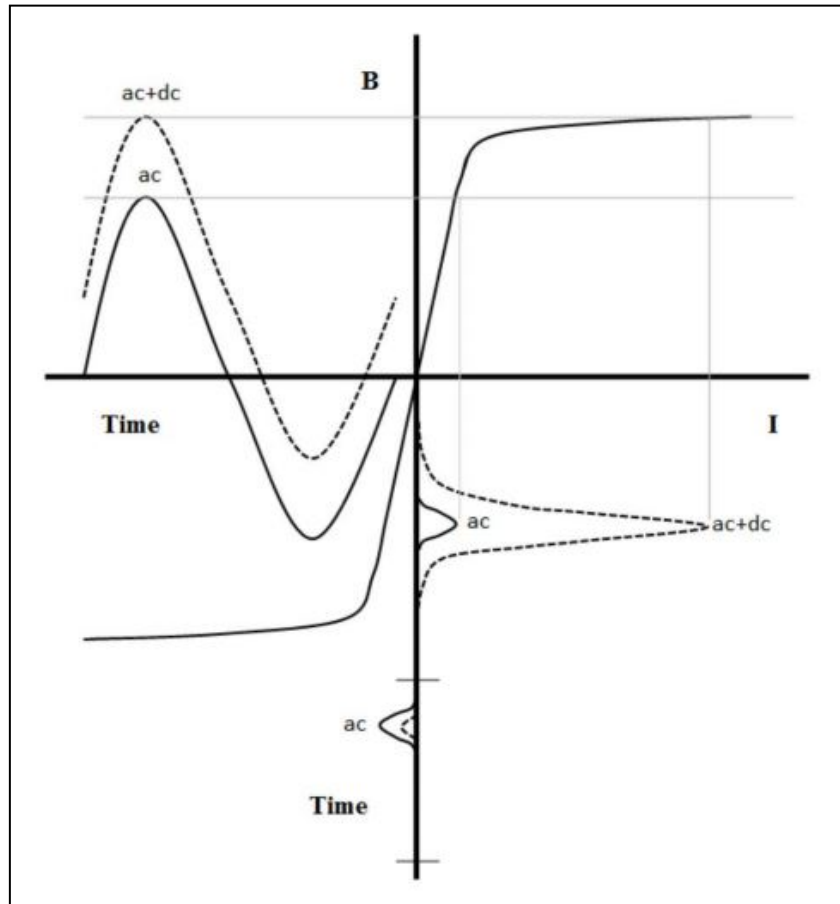


Figure 3.4, Effect of DC, Part-cycle (Half-cycle) saturation of transformer core [1].

The high-magnetizing currents, resulting from core saturation, will increase the amount of absorbed reactive power by the transformer. The reactive power (VAR) demand will experience an increase during the flow of GIC. The transformer magnetizing current pulse creates significant amounts of harmonics into the power system. Additionally, during the short duration of core saturation, due to the flow of GIC current in one winding, a lower voltage than rated voltage is induced in the other transformer windings of that phase resulting in an asymmetrical three-phase voltage condition [1].

The high magnitude of stray flux is produced from high magnetization current. This results in high eddy losses in the transformer windings, and structural parts of the transformer, causing corresponding increases in losses and temperatures. Also, as the core saturates, part of the main flux strays to tie plates, tank, windings, etc. causing higher losses and temperatures in these parts. However, due to the short duration of high level GIC pulses, the temperature rises in the windings and structural parts are much smaller than those calculated for DC current.

Additionally, as the core saturates, the pattern of the leakage flux changes causing higher circulating currents and winding overheating. This can happen at relatively low levels of GIC.

Other effects of part-cycle saturation are higher core sound levels, tank vibrations, and load sound levels during the GMD event. In addition, there is a significant increase in core losses during of the GIC pulse. If the core is not well designed to cool down substantially, the core hot-spot temperature will increase.

The above introductory remarks highlight the importance of studying the impact of GIC on power transformers. This thesis is an effort in that direction.

3.2 GIC Characteristics.

Fluctuations of solar radiation stream passing the earth's atmosphere might affect the earth's magnetic field, and thus GIC currents appear in the power network. The main characteristics of these currents are considered as very low frequency currents, thus viewed as Direct Currents, which might cause malfunctions in power network and lead to regional blackout, which can also incur large costs and risk to society.

The actual signature of GIC current that had been detected in March 1989, in Canada is illustrated in Figure 3.5. It shows that the GIC peaks occurred for a short period of time separated by many hours, where low to moderate levels were dominant. In term of transformers components thermal time constants, each GIC peak can be taken as an isolated event.

A GMD can last few days and continually generates the low frequency GIC currents (quasi-dc current), typically 0.01 Hz to 0.5 Hz. The common signature of the GIC current is low to moderate magnitudes of which lasts for several hours, interrupted by short-duration with high-peak pulses. Figure 3.5 shows an example of GIC signature made at the Ottawa magnetic observatory in Canada during the GMD that occurred on March 1989 [1].

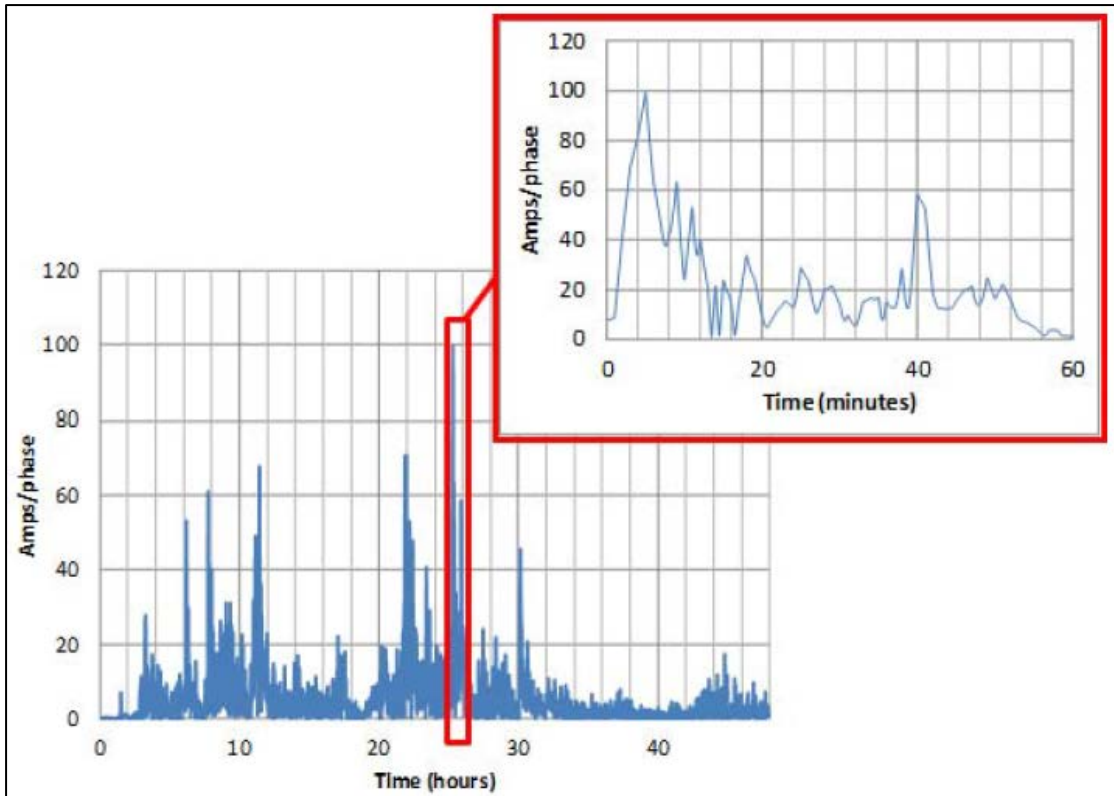


Figure 3.5, GIC profile at the Ottawa in Canada during the GMD that occurred in March 1989.

A simplified GIC signature, where GIC current is considered as a DC current for a short period of time is based on observation and study of large number of reported GIC events. For thermal evaluation of GIC effects on power transformer, each GIC level can be studied separately. The same has been proposed in NERC thermal assessment document [33].

The base and peak GIC level with their duration might be specified to the power transformer to be thermally evaluated. These parameters would be specified on the basis of system study of previously reported cases and response of the different transformers on the grid to a reference GMD event.

3.3 Effects of GIC on Power Transformers.

The main GIC effects on power transformer can be categorized under two main categories, core related and winding and structural parts related, as below:

1. Increased core losses, core noise, and core magnetizing current.
2. Increased load losses, the resistive and stray losses in windings and structural parts.

In the following sections, detailed effects of GIC phenomena on different transformer parts are discussed.

3.3.1 GIC Impact on Magnetic Induction

One of the main parameters that decide the size and cost of a transformer is the magnetic induction level. The higher the induction used, the smaller and cheaper the transformer will be. Transformers manufacturers tend to maximize the induction level of the core to the maximum allowed level, taking into account the followings limitations of finding out maximum nominal induction level:

- I. **Material Limitation:** The saturation value of the core material is a natural limitation in a transformer. A typical saturation level is between 2.0 and 2.05 Tesla. In practical life, the maximum nominal induction level is 1.85 T for Conventional Grain Oriented materials (CGO Material), and 1.9 T for High Induction grain-oriented materials (HiB Material).
- II. **Continuous Overvoltage Limitation:** The induction level has to be reduced according to a specified continues overvoltage's in standards or customers

specification. As a general rule, the nominal voltage over the maximum voltage multiplied by 2 Tesla will provide the maximum allowed induction for certain overvoltage level.

- III. **Time-limited Over-excitation Duration:** In many customers specification of generator transformers, a time-limited overvoltage duration is specified, for example, 120% over excitation for 60 seconds. Thus those short durations of over-excitation can be achieved only if the induction level is below a certain level, in this case 1.75 T [31].

In addition to all of above criteria, the highly expected GIC level that might be injected into transformers should be also taken into consideration. GIC current will cause a DC shift in operating nominal flux density. This might lead the core to saturation region, which in turns will force the transformer to draw high current with rich of harmonic contents. Furthermore, the volt per turn might also vary due to change of the operating flux density, as there is a direct relationship between the volt per turn and magnetic flux [31].

$$\frac{v}{t} = \frac{\pi}{\sqrt{2}} * A_c * B * \frac{f}{50} * 10^{-4} \quad (3.1)$$

Where:

$\frac{v}{t}$: Volt per turn (V/turn).

A_c : Core leg cross sectional area (mm²).

B : Core leg induction level (T).

f : Frequency (Hz).

The magnitude of additional DC flux will be determined by three main factors: the magnitude of the GIC current, number of turns in which the GIC current will flow, and the reluctance of the path of the DC flux as per the following equation (3.2).

$$\phi_{dc} = \frac{N * I_{gic}}{\mathcal{R}} \quad (3.2)$$

Where:

ϕ_{dc} : DC flux shift.

N : Number of turns.

I_{gic} : GIC current (A).

\mathcal{R} : Reluctance.

The reluctance value is not a constant and it depends on the level of core saturation. It depends on the magnitude of permeability (the permeability itself is a function of magnetic flux intensity (H)), as per below Figure 3.6.

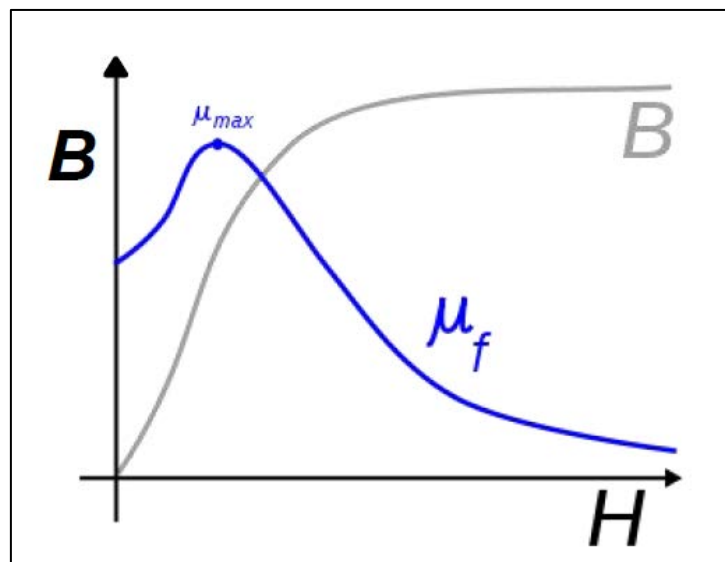


Figure 3.6, Permeability of core in function of BH curve.

3.3.2 GIC Impact on No-Load Current

The no-load current represents the value of current that is required to magnetize the magnetic core. In normal condition, the transformer iron core provides a low reluctance path to the magnetic flux density. The magnetization current is quite low value. It is in the range of 2% of full load current. Most of the magnetic flux will pass through the core [29].

No-load current is usually calculated based on empirical factor derived from test results, which is VA/kg (Volt-Ampere required per kg of material) versus induction level in Tesla. This factor is provided along with each core material card. Equation (3.3) is used to calculate the core excitation current.

$$I_{m\%} = \frac{[VA/kg] * W_c}{MVA} \quad (3.3)$$

Where:

I_m : Excitation current as a percentage of the nominal current.

$\left[\frac{VA}{kg}\right]$: Exciting power factor, a function of the core material.

W_c : Total core weight (kg).

MVA : Base MVA power.

No-load current is peaky in nature and rich of harmonics, due to non-linearity of BH curve (magnetization curve). For Cold Rolled Grain Oriented (CRGO) material the fundamental component is 1 per unit, 3rd harmonic is 0.3 to 0.5 per unit, 5th harmonic is 0.1 to 0.3 per unit and 7th harmonic is max 0.1 per unit [29]. The harmonic contents do not contribute to increasing of copper losses, except during extreme level of core saturation. During GIC event, VA/kg parameter is increased due to the shift of operating flux density to a higher value.

3.3.3 GIC Impact on No-Load Loss and Core Temperature Rise

The no-load or excitation losses represent the power that is absorbed by the transformer core when rated voltage and rated frequency are applied to one of the winding whereas the other winding is left open-circuited. Core loss includes mainly hysteresis and eddy current losses of the core. In addition to resistive losses of conductor due to excitation current. No-load loss is usually calculated based on empirical factor derived from test results, which is W/kg (watt per kg of material) versus induction level in Tesla. This factor is provided along with each core material card.

No-load loss, the eddy loss (P_e) and hysteresis loss (P_h) are given by [29]:

$$\text{No load loss} = Wt K_b w \quad (3.4)$$

$$P_e = k_1 f^2 t^2 B_{rms}^2 \quad (3.5)$$

$$P_h = k_2 f B_{mp}^n \quad (3.6)$$

Where:

K_b : Core building factor.

Wt : Core total weight.

P_e : Eddy loss.

P_h : Hysteresis loss.

k_1, k_2 : Constants which depend on the material.

B_{rms} : Effective flux density, RMS value.

B_{mp} : Actual peak value of the flux density.

n : Steinmetz constant.

t : Thickness of individual lamination.

Surface and center temperature rise has a direct relationship with core losses. Temperature rise limit for the core is 120°C for the core surface temperature, and 140°C for the core hotspot (highest temperature in the core). The core material can withstand temperatures in the range of 800°C (annealed temperature of core lamination during manufacturing), but the low temperature rise limit comes from the insulation of core laminations, pressboard insulation (class A: 105°C) and core bolt insulation (class B: 130°C) that may get damaged.

3.3.4 GIC Impact on Transformer Noise Level

Magnetostriction of core laminations is the main cause for the no-load noise. When transformer works at low magnetic induction level, the noise level will also be low. On the other hand, increasing the operating magnetic induction will increase the noise level of transformer. Winding and cooling system are the other sources of transformer noise. NEMA-TR1, Sound levels in transformers and reactors standard govern the allowed sound level of transformer [32].

Magnetostriction is with the direct relationship with magnetic induction level. The main noise comes from core yoke as the core limb noise is damped by winding materials. The quality of the yoke clamping has a significant influence on the noise level. Other factors which decide the noise level are: operating flux density, core material type, core weight, and operating frequency. The reduction of flux density by 0.1 T, the noise level will be reduced about 2 dB. The operating peak flux density and core weight are the main two factors to determine the noise level. The change in noise level as a function of these two factors can be expressed by equation (3.7) [29].

$$\Delta L = 10 \log \left[\left(\frac{B2}{B1} \right)^8 \left(\frac{W2}{W1} \right)^{1.6} \right] \quad (3.7)$$

Where:

ΔL : Change in noise level.

$W1, W2$: Core weights.

$B1, B2$: Operating peak flux density.

3.3.5 GIC Impact of Reactive and Active Power Losses

Increased reactive power demand in power system is one of the important indicators of the GIC flow in power system through grounded transformers. The larger the magnetization current, the larger consumption of reactive power by transformers. The relation between the increased GIC currents and absorbed reactive power by grounded transformers will be investigated in this thesis, using PSCAD tool.

Additional conductor's resistive losses (due to ohmic resistance of windings) will increase due to the injection of GIC currents into the transformer.

Additional stray losses (eddy current losses) and increased axial and radial magnetic leakage fields: The stray losses of the transformer can be classified into two major parts. The one in windings and the one in steel structural. The winding stray losses can also be further classified into two main categories: eddy current losses and circulation current losses. The eddy current losses occur due to leakage magnetic field in windings. The eddy current loss in windings increases due to the increase in conductor dimensions. Hence, the winding conductor that exposed to high radial and axial leakage

field is usually subdivided into smaller one. Figure 3-7 shows the leakage field incident on a winding conductor.

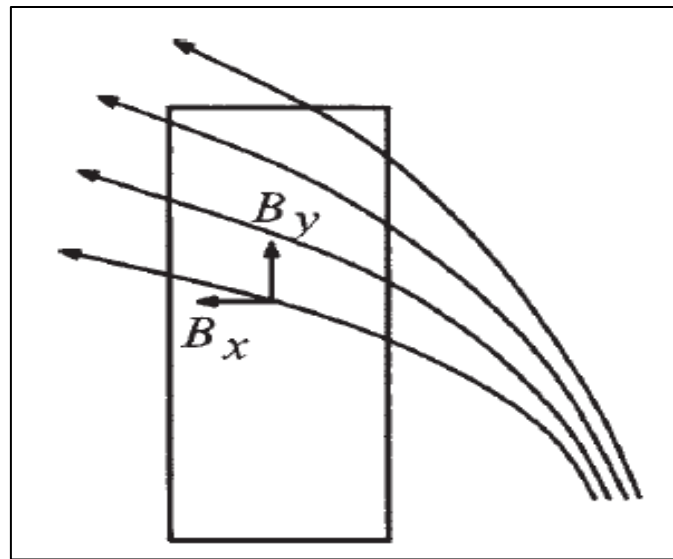


Figure 3.7, Leakage field components on winding conductor.

FEM analysis is performed to obtain those two components of magnetic leakage flux B_x and B_y . Equations (3.8) and (3.9) are used to calculate the associated losses with those components [29].

$$(Pe)_{axial} = \frac{\omega^2 B_y^2 t^2}{24\rho} \quad (3.8)$$

$$(Pe)_{radial} = \frac{\omega^2 B_x^2 w^2}{24\rho} \quad (3.9)$$

Where:

P : Eddy loss per unit volume.

B_x, B_y : Radial and axial flux density components.

t, w : Thickness and width of conductor.

ρ : Resistivity.

3.3.6 GIC Impact on Winding Temperature Rise and Hot Spot Creation

The flow of GIC current through power transformers can cause part-cycle saturation, forcing the flux to flow outside of the core and between the windings. When core saturates, the air flux and exciting current might have high harmonic content which increases the eddy losses and temperature rise in windings and structural parts.

To avoid hot spot creation in the windings due to leakage fields, a proper conductor dimensions should be selected based on the knowledge of flux density distribution within a winding. Many transformer manufacturers tend to subdivide winding conductors into a number of parallel conductors to reduce the eddy loss, specifically due to high radial leakage field. If the conductor thickness (t) is subdivided into two exact two parallel conductors with $(t/2)$ thickness, the eddy loss will be reduced by a factor of $1/4$ [29].

The radial flux is perpendicularly incident on the axial conductor dimension on the top and bottom of the winding. The stray loss is highly expected on those locations, the exact allocation of those places will be through detailed FEM analysis. The Continuously Transposed Conductor (CTC) is also can be used for a few top and bottom disks to minimize the eddy loss, whereas the remaining disks can be made of normal strip conductor.

The thermal time constant plays a significant role in determining the GIC effect (temperature increase), as the peak values of GIC are only sustained for a short period of time.

Table 3.1 shows the thermal time constant for the major transformers materials that can be affected by GIC current. There will be an insignificant increase in core and oil temperatures as their time constants are larger than windings materials thermal time constant.

It has been assumed that the GIC current will sustain for the time period more than the thermal time constants of winding (15 minute) and core (2 hours), to find out the increased temperature rises.

Table 3.1, Thermal time constant for main materials [29]

Materials	Thermal Time Constant
Windings	10 to 15 min
Core	1 to 2 hours
Transformer Oil	8 to 10 hours

3.4 Historical GIC Cases.

The sun has solar activities that occur all the time, but every 11 years (on an average) these activities peak occur. There have been many reported significant GMD events that forced the transformers to be taken out of service for some weeks, and in some cases caused a blackout for a few hours in many substations worldwide, Table 3.2 is summarized the main reported cases since 1989.

Table 3.2, Main Reported Transformers Damage / Over-Heating Contributed to GIC [12], [14], [20].

Reported Case No.	Year	Location	Description of Disturbances caused by GIC
1	1989	Hope Creek Nuclear Generating Station, in Salem County, New Jersey, United States.	<ol style="list-style-type: none"> 1. Significant overheating in windings of shell-form transformers. 2. Significant gassing detection after a week. 3. Tank paint discoloration.
2	1989	Hydro Quebec Electricity Transmission System in Quebec, Canada.	<ol style="list-style-type: none"> 1. Eight hours blackout of HQ system.
3	2003	South Africa	<ol style="list-style-type: none"> 1. Windings Damaged due to Significant overheating in over insulated main windings leads.
4	2003	Sweden	<ol style="list-style-type: none"> 1. 20-50 minute blackout due to system instability. 2. Minor heating and gassing also reported in transformers.

The main reported GIC events in Manitoba Hydro high voltage transmission network have been presented in [12]. On-line continuous monitoring system for GIC currents has been used to record all occurred phenomena. Those events include the peak seasons of solar cycle 23 and solar cycle 24. At the end of this paper, some mitigation techniques have been proposed to overcome such a phenomena.

Manitoba Hydro high voltage networks are located in high geomagnetic latitude zone where it might be frequently exposed to moderate to high levels of geomantic disturbances. The on-line continuous monitoring system project started in 1992 by installing the monitoring equipment's in Winnipeg and then in Grand Rapids, the project is called EPRI SUNBURST. Those monitoring equipment use the transformers grounded neutrals to identify the GIC currents.

During solar cycle 21, the maximum reported GIC value was 105 A in 500 kV transmission lines. Three protection relays operated and the 500 kV lines tripped. In solar cycle 22, a several GIC events were captured between 1992 to 1993, specifically in 10th September 1992. The maximum recorded GIC current was 45 A in 500 kV lines, which was rich of 5th harmonics contents. In solar cycle 23, between 2000 and 2001, the highest GIC current as 67A in 15th July 2000. While in solar cycle 23, in 2012, the maximum reported current was 21A in March and July 2012 [12].

After investigating the reported cases in Manitoba, it can be concluded that GIC currents exist most of the time in high voltage transmission lines entering through power transformer ground neutral points, but with varying levels depending on the severity of the sun activities, which reach the peak every 11 years on an average.

Based on this study on Manitoba high voltage networks, the specification of all installed equipment, specifically power transformers, have been updated to take those GIC levels into account. The basic mechanisms of affecting high voltage networks by geomagnetic storm is shown in Figure 3.8.

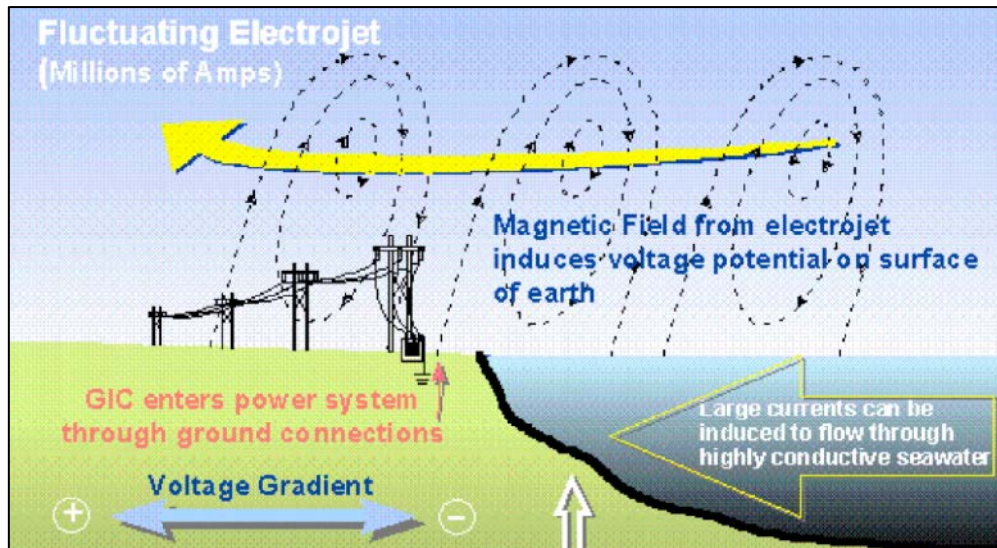


Figure 3.8, Principal mechanisms of GMD coupling with high voltage network [13].

The average GIC levels as a function of transmission network voltage level have been illustrated in [13], it is noted that 765 kV transmission system might have 6 times of 138 kV transmission system for the same GMD conditions, mainly (1 V/m). This is due to network resistance. This comparison has used the average US resistances.

Furthermore, a magnetic density in (nT) has been given in time and space across North America at one instant of time during the geomagnetic disturbance of October 1991, as shown in Figure 3.9 [13].

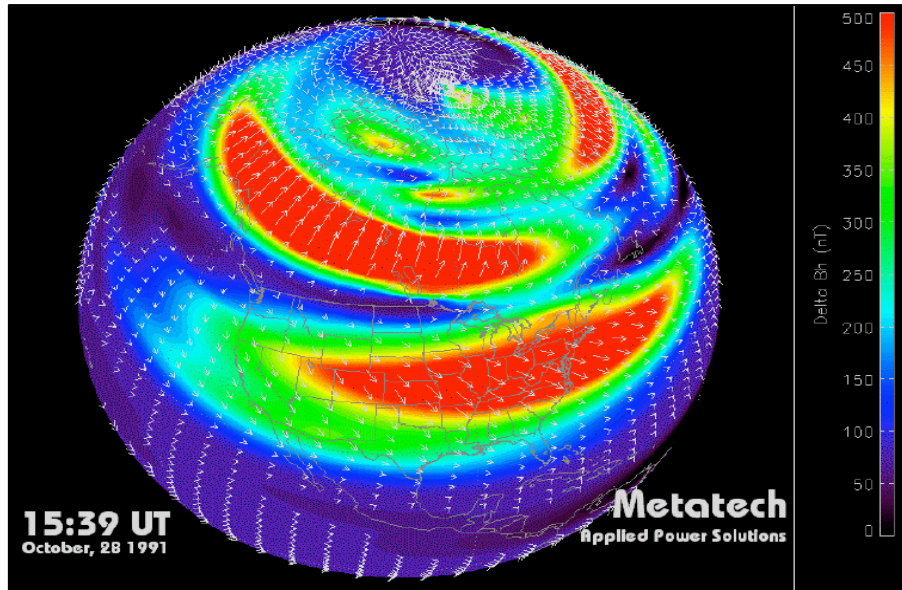


Figure 3.9, Magnetic density in nT across North America during GMD in October 1991 [13].

Most of Chinese substations have a single phase power transformer, which makes the Chinese network much more vulnerable to the GMD. During the 23rd solar cycle, GIC values have been measured at Ling'ao nuclear power substation in Guangdong, Jiangsu and many other places in China. The maximum measured GIC current is less than 75 A [15].

In China, solar storm impacts become a significant issue after the solar cycle 23, in 2001. Especially with building the UHV system 1000 kV system. The risk assessment has been made for 1000 kV based on historical data and estimated new network model.

In 2005, 750 kV Chinese power grid has been constructed in the north-west of China. The GIC values have been calculated using the collected geomagnetic data and the Chinese earth conductivity model. The maximum GIC current in 750 kV is found to be 102 A, which is 35% increase of that in 500 kV. So for 1000 kV, the GIC values might exceed 200 A, this is high and dangerous value if the installed equipment in this network is not designed to withstand and survive against such a phenomena [15].

The followings country-wise main historical reported occurrences of GMD and their impact of electrical power system network have been shortlisted in coming sections:

- **Canada/US:**

Hydro Quebec 735 kV power network was subjected to the GMD on March 13, 1989. The whole transmission network and power transformers were affected by the flowing of GIC current. This in turns caused transformer saturation, increased current harmonics and consequently increased the reactive power consumption of saturated transformers, lead to severe voltage regulation problem and loss many static compensators, in addition to tripping of several 735 kV lines. Such cascaded problems lead to drop in frequency and voltage level throughout the system. The system operators failed to restore the balance between available generation and system loads. The lost capacity was too large causing a blackout for about 9 hours [14].

Other North American utilities, specifically in the eastern region of US, felt the disturbance, but not with the same severity level of what happened in Hydro Quebec. During the disturbance, some of the installed capacitors were lost due to high harmonic current content, which causing incorrect operation of relays.

A step up generator transformer 22/500 kV installed in Salem nuclear plant in New Jersey, south of Philadelphia had been damaged due to overheating. Other transformers were removed from service due to high detected gassing in oil, or sign for un-usual core and tank heating. The investigation showed that 80 A of GIC current was injected into transformers during GMD causing all of above troubles [14], [20].

- **Sweden:**

The main GMD occurred in Sweden was during cycle 23, peaked in 2000, where the most significant impact was felt in Northern Europe. The Swedish high voltage power transmission system was exposed to unusual high geomagnetic disturbance. Many lines of 220 kV and 400 kV tripped. Many transformers of 400/220 kV were overheated and some of them disconnected [14], [20].

Another geomagnetic disturbance in Sweden lasted for about two days with causing many cascaded problems and failures. It started on 29 October 2003 by disconnecting 220 kV power line. Cascaded effect disconnecting the 400 kV power line that connecting Sweden with Poland, causing an interruption of 300 MW imported to Sweden. On the second day, many transformers of 400/220 kV and 400/130 kV were disconnected due to overheating and overloading, leading to blackout for about 50 minute on more than 50,000 customers in Malmo [20].

- **UK:**

Significant GIC effects during the geomagnetic storm in 1989 have been reported in UK electricity supply system. The main affected cases can be summarized as follow: large reactive power demand, voltage regulation exceeded 5%, failure of 400/132 kV power transformers in some substations and high level of current harmonics due to transformers saturation. The maximum recorded GIC current was 25A [20].

- **South Africa:**

South Africa is located in an intermediate latitude against GMD and many transformers are equipped with DGA (Dissolve Gas Analyzer). In 2003 magnetic storm, many transformers were overheated. After some time from the occurred GMD, many

transformers tripped due to excessive gassing detected by the DGA in 2003 and 2004, and some of the transformers were removed from service due to insulation damage, that most probably were breakdown due to excessive temperature rise. The probability of transformer failure would increase after each geomagnetic storm. The maximum recorded GIC current as 10A [20].

- **China:**

During 23rd solar cycle, many GIC data have been recorded in Guangdong, Jiangsu and other regions of China. The measured peak GIC levels at the 500 kV transformer neutral point in Ling'ao nuclear power substation and in Guangdong during two magnetic storms in November 2004 were 47.2 A and 75.5 A respectively [15]. The impact of strong GMD on power network becomes a significant issue due to introduce the 1000 kV UHV system, which has much lower resistance values compared with existing 500 kV and 220 kV.

The main GIC reported cases from 1989 to 2015 have been summarized as per below Table 3.3. It is true that the sun has solar activities peak every 11 years on an average (eleven-year solar cycle and the years 2012-2014 have been associated with a solar activity peak).

Table 3.3, Main GIC reported cases from 1989 to 2015.

Case No.	Date	Location	Recorded Highest GIC (A)	Reference No.
1	13-Mar-89	PSE&G Salem Generating station, USA.	95	[2]
2	13-Mar-89	Manitoba Hydro Quebec, Canada.	80	[14], [12]
3	13-Mar-89	United Kingdom (UK).	25	[14]
4	13-Mar-89	Ottawa, Canada	100	[18]
5	19-Oct-89	United Kingdom (UK).	25	[3]
6	21-Feb-91	Forbes Substation in Minnesota, USA.	6	[13]
7	28-Oct-91	Brighton, USA.	30	[13]
8	28-Oct-91	Chester, USA.	44	[13]
9	28-Oct-91	MYA, USA.	42	[13]
10	28-Oct-91	PLV, USA.	60	[13]
11	28-Oct-91	So. Canton, USA.	31	[13]
12	8-Nov-91	United Kingdom (UK).	25	[14]
13	15-Jul-00	Jefferson substation, USA.	90	[19]
14	15-Jul-00	Kammer Substation, USA.	40	[19]
15	15-Jul-00	Jackson's Ferry substation, USA.	38	[19]
16	29-Oct-03	Southern Sweden.	330	[14], [20]
17	29-Oct-03	South Africa.	10	[14]
18	9-Nov-04	Ling'ao Power Plant, China.	60	[15]
19	14-Feb-11	Southern Manitoba, Canada.	8.4	[20]
20	22-Mar-15	Australian, British Columbia, Canada	3	[16]

CHAPTER 4

PROBLEM FORMULATION AND METHODOLOGY

4.1 Problem Formulation

During any GMD event, which has a cycle of 11 years on an average, the magnetic fields of the earth is disturbed as described in Chapter 3. Such magnetic field disturbance will create an induced voltage in the closed loop of transmissions lines and grounded transformers. This causes the GIC current to flow and enter the power transformers from their grounded neutral points. The GIC currents are viewed as DC current. From its signature, the GIC peaks occur for a short period of time separated by many hours, where low to moderate levels are dominant. Each GIC peak can be taken as an isolated event and studied separately.

In this thesis, the transformers affected parts and performance by GIC phenomena will be studied as follows:

- I. Core Magnetic Induction: GIC will cause a DC shift in operating nominal flux density. This might drive the core into saturation region. Which in turns will force the transformer to draw high current rich of harmonic contents. The exact induction shift will be simulated and obtained by Finite Element Method (FEM) analysis.
- II. No-Load Current and its distorted shape: Shifting the operating flux density into the saturation region will lead to higher magnetization current, and destroy the no-load current waveform, which is peaky in nature and rich of harmonics. PSCAD tool will be utilized to study the magnetizing current shape.

- III. No-Load Loss and Core Temperature Rise: The hysteresis and eddy current losses of the core, in addition to resistive losses of the conductor due to additional drawn excitation current will be also affected by GIC current. The losses will be calculated for each GIC level.
- IV. Transformer Noise Level: As a result of the shifting of operating induction level the transformer sound level will increase. The exact figure of increase in noise level will be calculated for each GIC level.
- V. Reactive Power Consumption: The larger the magnetization current, the larger consumption of reactive power by transformers. The relation between the increased GIC currents and absorbed reactive power by grounded transformers will be investigated in this thesis, using PSCAD tool.
- VI. Additional Resistive Losses: GIC current and additional magnetization current is drawn by transformer during part-cycle saturation will also have a negative impact on the increase of resistive losses. Percentage increase will be calculated for each GIC level.
- VII. Additional Stray Losses: The eddy current losses occur due to leakage magnetic field in windings. The exact leakage field will be obtained using FEM analysis, then to calculate the associated losses with those leakage components.
- VIII. Winding Temperature Rise and Hot Spot Creation: As a result of increased losses, the temperature rise of windings will rise. The exact allocation of hot-spot places will be obtained through detailed FEM analysis.

In this thesis, the following methodology will be adopted to evaluate the GIC effects on power transformers:

- I. Flux Density Shift: Due to GIC injection through transformers grounded neutrals, the operating flux density will be shifted. The study will be applied on a widely used Saudi transformer 40/50/60 MVA, 132/13.8 kV, YNyn0. This transformer has the rated operating flux density of 1.606 T. The core is Cold Rolled Grain Oriented (CRGO). As the GIC value increases the flux density peak increases. However, due to non-linearity nature of magnetizing B-H curve of the core material, the material permeability is limiting the increase in flux density in a linear way. The DC flux can be calculated by dividing the Ampere-Turn over the Reluctance. FEM analysis will be performed to find out the exact shift of flux density.
- II. Core Losses and Core Noise: As a result of the increase in magnetic flux density in the core, both core losses and core noise magnitudes will significantly increase.
- III. Magnetizing Current: As a result of core half-cycle saturation, high magnitude with short duration magnetizing current will be drawn by the transformer. This represents a corresponding increase in reactive power absorbed by transformers. In addition to the injection of current harmonics in power system.
- IV. Load Losses: Mainly can be divided into two parts, additional losses in windings (ohmic and eddy current), and additional losses in structure parts of the transformer. Due to high magnetizing current and its shape, higher magnitudes of leakage flux will be produced. Thus higher eddy current losses in the windings and transformers structural parts will be experienced.

- V. Allocation of expected hot spot creation in windings, core, clamps and steel structures will be investigated and solutions will be proposed to overcome such hot spot to a certain GIC level.
- VI. Simulation of GIC effects on power transformer under additional overloading conditions.
- VII. Cost impact of enhancing power transformers to withstand some certain level of GIC will be investigated at the end of this thesis.

Table 4.1 shows the details of the 60 MVA transformer (132/13.8/6.6 kV, YNyn0+d1). HV winding is a star connected with the solidly grounded neutral point. HV winding consists of three main parts: main HV winding, coarse and fine regulating windings. The core diameter is 575 mm with window height 1542 mm and leg center to center of 1379 mm, further details of the core are tabulated in Table 4.2.

Table 4.1, 60 MVA, 132/13.8 kV transformer main windings parameters.

Winding	TV	LV	HV_Main	HV_Coarse	HV_Fine
Type	Single layer	Multilayer	Countershielded Disc	Single layer	Tap disc (Interleaved)
Conductor Type	CTC	CTC	Rectangular	Rectangular	Rectangular
Number of Turns	66	80	623	110	110
Radial build (mm)	16.5	77.5	92.5	14	24
Winding Height (mm)	1301	1311	1273	977	876
Top Clearance (mm)	146	141	148	308	359
Bottom Clearance (mm)	95	90	121	257	307

Table 4.2, 60 MVA, 132/13.8 kV transformer main core parameters.

Core Material	Core Diameter (mm)	Window Height (mm)	Leg Center to Center (mm)	Main leg Cross section (mm ²)	Widest Sheet (mm)	Core weight (kg)
M080-23P5-DR	575	1,542	1,379	232,565	570	20,213

The transformer core is made by steel grade of M080-23P5-DR. the specific total loss at 1.7 T at 50 Hz is 0.8 W/kg and magnetic polarization of 800 A/m is 1.91 T. the nominal thickness of the sheet is 0.23 mm. 60 MVA three phase power transformer is three limb core type, where no outer limbs for flux return exist. The zero sequence flux will be close though core clamps, tank wall and air surrounding the core. Hence the reluctance value for zero sequence flux is very high in three limbs core type. This in turns minimizes the change in flux change and provide less sensitive design to GIC phenomena.

It is difficult to get a closed-form solution for a problem such as a magnetic problem in a transformer. However, the problem can be broken down into a large number of regions. Each with simple geometry (in our case triangles) where the differential equations can be utilized in a much easier way. This is the idea of finite element analysis, where the problem domain is subdivided into a large number of small elements, through the process of discretization. Specifically, FEMM discretizes the problem domain using triangular elements. For each element, the solution is approximated by a linear interpolation of the values of potential at the three vertices of the triangle. The linear algebra problem is formed by minimizing a measure of the error between the exact differential equation and the approximate differential equation.

4.2 Magnetic Problem in FEMM

In magnetic problem in FEMM tool, the boundary conditions are in Dirichlet type, where the value of a magnetic vector potential (A) is defined on the boundary. Commonly, the Dirichlet-type boundary conditions in magnetic problems is to define $A = 0$ along a boundary to keep magnetic flux from crossing the boundary [38].

The magnetic solver in FEMM utilizes Maxwell's equations. In our case, which considered as a low frequency problem, the displacement current is ignored. The magnetic field intensity (H), magnetic field density (B) and magnetic vector potential (A) are related to each other by the following equations [38]:

$$\nabla \times H = J \quad (4.1)$$

$$\nabla \cdot B = 0 \quad (4.2)$$

$$B = \mu H \quad (4.3)$$

$$\mu = B / H(B) \quad (4.4)$$

$$B = \nabla \times A \quad (4.5)$$

Where:

H : Magnetic field intensity.

B : Magnetic field density.

μ : Permeability

A : Magnetic vector potential.

All of above-affected transformer parts and performances are studied using three types of models, two FEM analysis, and one PSCAD simulation as per Section 4.3.

4.3 Transformer FEM Models.

4.3.1 Model No.1 (Induction Model).

The main purpose of this FEM Model is to simulate the exact shift of new operating flux density due to entering different GIC currents into HV winding transformer through its grounded neutral. The magnitude of the additional DC flux can be obtained by two methods. The analytical method as per equation (4.6). It shows that the DC flux shift is governed by three main factors: the magnitude of the GIC current, number of turn (N) in which the GIC current will flow, and the reluctance (R) of the path of the DC flux.

$$\phi_{dc} = \frac{N * I_{gic}}{\mathcal{R}} \quad (4.6)$$

Where:

ϕ_{dc} : DC flux shift.

N: Number of turns.

I_{gic} : GIC current.

\mathcal{R} : Reluctance.

The analytical method is the easiest method if a fixed value of reluctance is considered. However, the core reluctance value is not constant and it depends on the level of core saturation. Specifically, it depends on the magnitude of permeability, which itself is a function of flux intensity (H A.t/m). The above equation will not provide the accurate DC shift, as a new reluctance value for the case should be considered.

To resolve this issue and get accurate DC shift of flux density at different GIC currents levels, a detailed structure of transformer active part (core and windings) enclosed by

tank border has been built using FEMM tool, as illustrated in Figure 4.1. The non-linear characteristic of magnetic core has been also considered in this model. The BH curve of transformer core has been defined as shown in Figure 4.2.

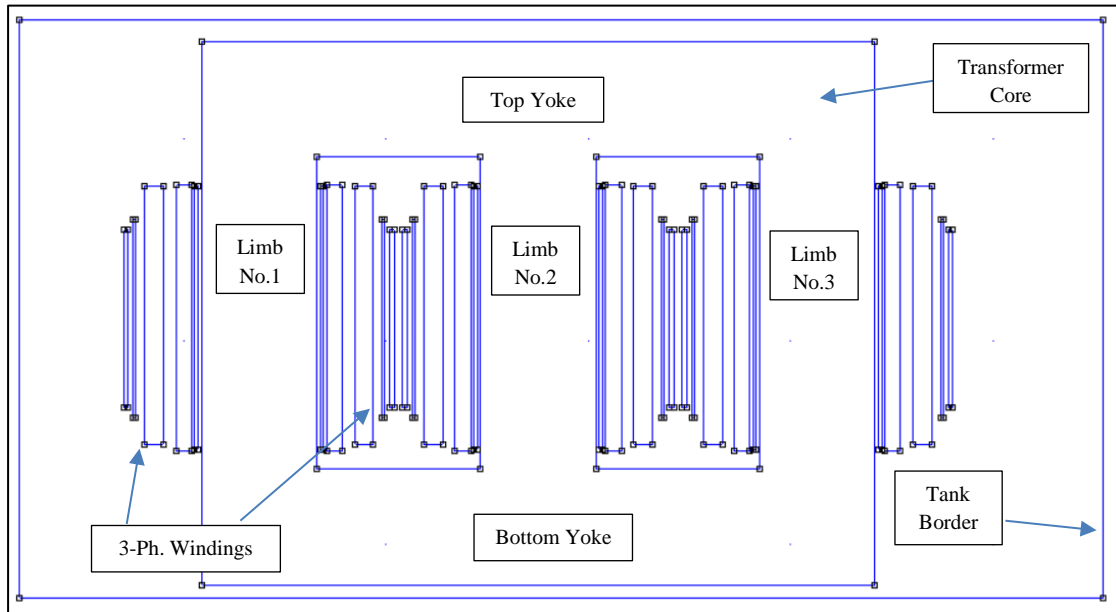


Figure 4.1, Model No.1 (Induction Model).

The model consists of laminated sheet three limbs core, top and bottom core yokes, three phase windings (LV and HV) enclosed by transformer tank, which is filled by oil. The geometry was drawn by AutoCAD and imported by FEMM with scale for accurate analysis. The details of windings (type, direction and number of turns) and circuit connection have been also defined in FEMM according to reference 60 MVA transformer.

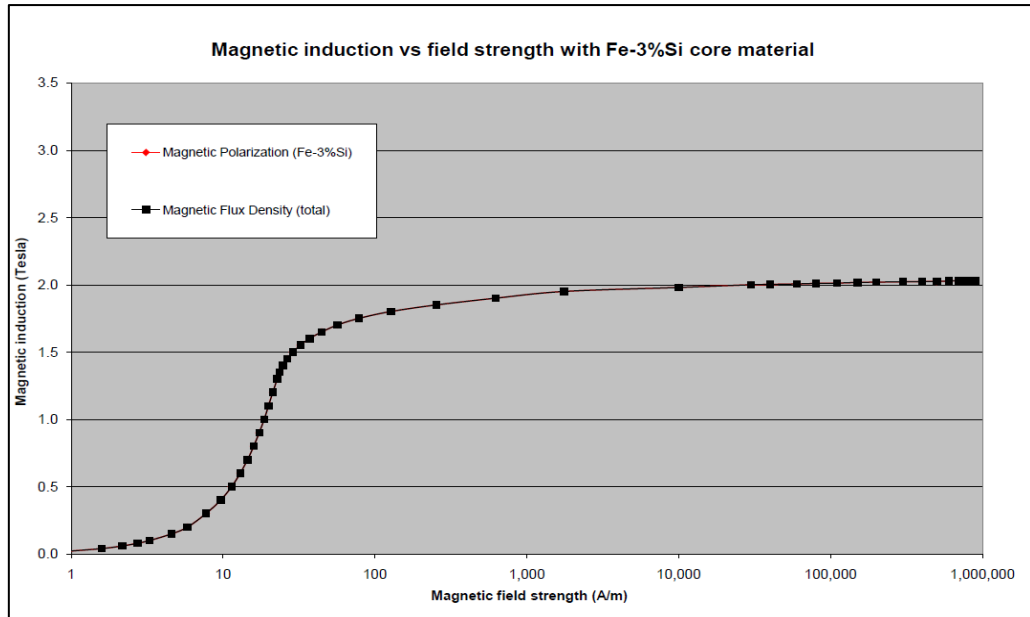


Figure 4.2, Magnetization Curve of M080-23P5-DR core grade (BH Curve) [30].

The following cases will be simulated using Model No.1 “Induction Model”:

- **Case No.1:** The no-load condition, with nominal flux density, with different GIC currents (50, 100, 150, 200, 250 and 300 A) into transformer HV neutral point.
- **Case No.2:** The no-load condition, with 90% of nominal flux density, with different GIC currents (50, 100, 150, 200, 250 and 300 A) into transformer HV neutral point.
- **Case No.3:** The no-load condition, with upgraded core material type with nominal flux density. Different GIC currents will be injected (50, 100, 150, 200, 250 and 300 A) into transformer HV neutral point.
- With each above cases, no-load current, no-load loss, core temperature rise and increased sound level are found at each GIC level.
- The above cases will be repeated with the additional cooling channel in core to enhance its cooling efficiency.

- **Case No.4:** Simulate the DC shift with different GIC current with reduced HV winding turns.

4.3.2 Model No.2 (Stray Losses Model)

The main purpose of this model is to allocate the extreme leakage magnetic flux and to obtain the exact axial and radial leakage flux components, which will cause the eddy current losses in transformer windings, clamping, and steel structure. Magnetic leakage flux already exists outside core and between the windings in normal operating conditions. This is represented by transformer reactance. However, due to part-cycle saturation during the GIC phenomena, the leakage flux will increase and might create a hot-spot, especially in the winding as it has the lowest thermal time constant, 10 to 15 minutes, as the peak values of GIC are only sustained for a short period of time. There will be an insignificant increase in core and oil temperatures as their time constants are much bigger values, in hours.

A detailed cross-sectional one leg windings and core clamps are built using FEMM tool as shown in Figure 4.3. The windings from innermost are the LV winding, the HV main winding, HV coarse and fine regulating windings. The core top and bottom clamps are defined as mild steel. All the surrounding medium elsewhere are defined as an oil.

In addition to defining the materials characteristics of each part in cross-sectional view, the number of turns and circuit connection have been also determined as shown in Table 4.1. The HV main, HV coarse and HV fine are connected in series. The extreme positive tap position where all HV winding turns are in has been considered in our simulation.

The following cases will be studied using Model No.2 “Stray Losses Model”.

- **Case No.1:** The full-load condition, with nominal operating conditions, with different GIC currents (50, 100, 150, 200, 250 and 300 A) into transformer HV neutral point.
- **Case No.2:** The overload load condition (120%), with different GIC currents (50, 100, 150, 200, 250 and 300 A) into transformer HV neutral point.
- In each case the extreme allocation of leakage flux and exact axial and radial leakage flux components will be obtained. The corresponding losses will be calculated using equations (3.8) and (3.9), where the eddy current losses is directly proportional to the squared of leakage flux components (axial and radial).
- Winding temperature rises will be simulated with each of the above cases.

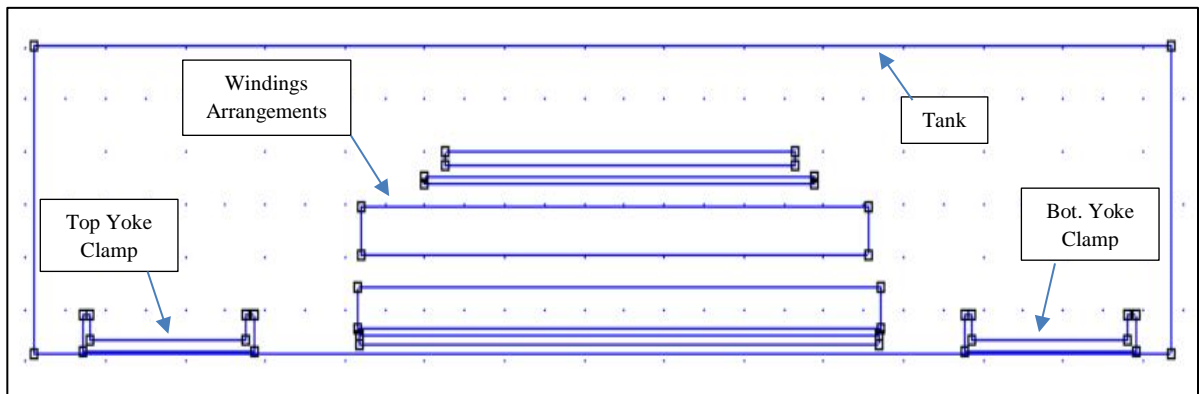


Figure 4.3, Model No.2 (Stray Losses Model).

The model consists of windings, core clamps and core and tank boundary. The top and bottom core clamps are defined as mild steel. The geometry was drawn by AutoCAD and imported by FEMM with scale for accurate analysis. The details of windings (type, direction and number of turns) and circuit connection have been also defined in FEMM according to reference 60 MVA transformer.

Figure 4.4 shows the flow chart of Model No.1 (Induction Model) and Model No.2 (Stray Losses Model). Where the new operating flux density, no-load current, no-load loss, magnetic leakage flux components, stray land resistive losses and temperature rises will be obtained.

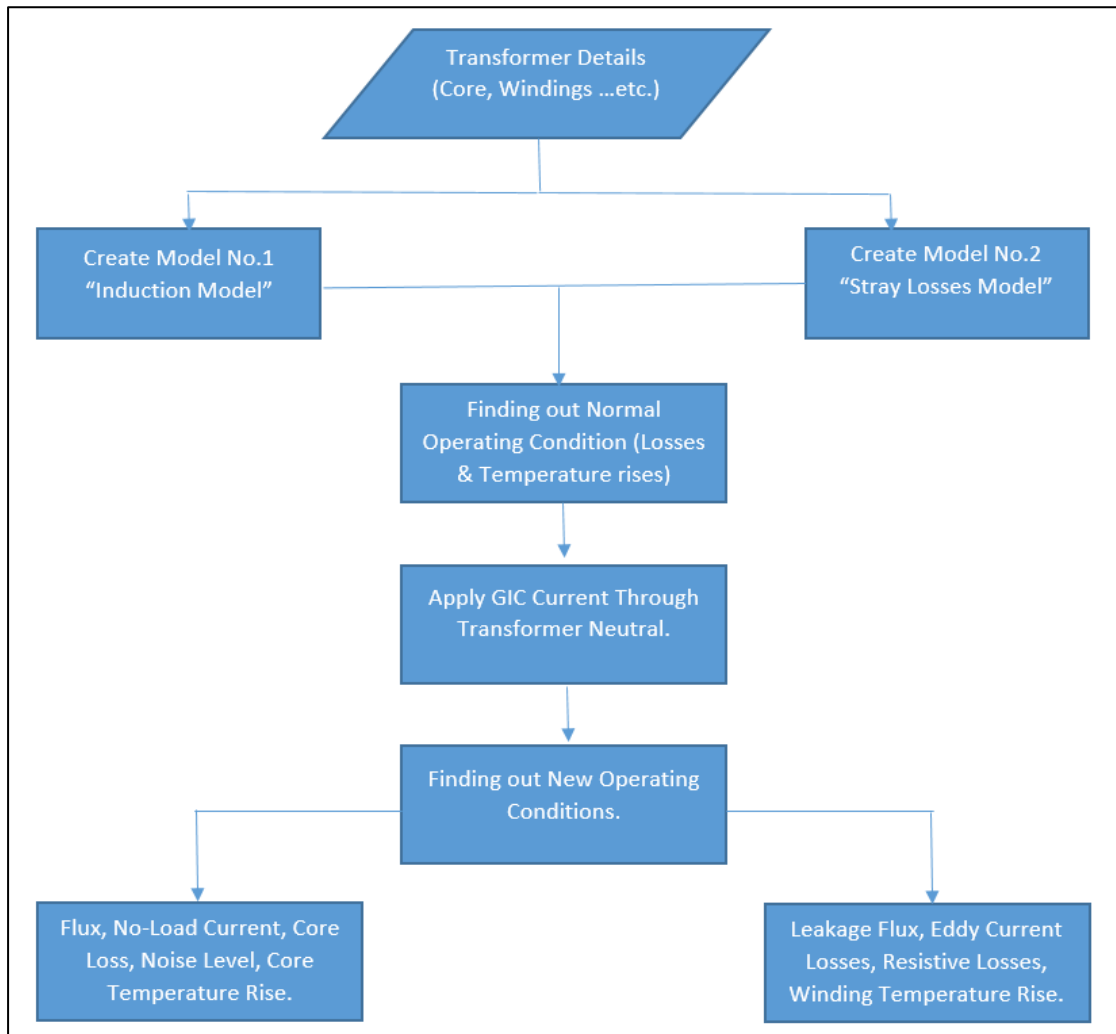


Figure 4.4, Flow Chart of Model No.1 and Model No.2.

4.3.3 PSCAD Model.

The main purpose of this model is to simulate the behavior of transformer during different GIC levels. GIC current will be injected through the grounded neutral. VAR consumption, current waveform shape of magnetization current will be studied at different GIC levels.

In order to investigate the relationship between reactive power losses and GIC magnitude, 60 MVA three-limb power transformer has been used for simulation of GIC in PSCAD. The transformers most likely to be exposed to GIC are step-up and step-down transformers connected to long transmission lines. PSCAD model is shown in below Figure 4.5.

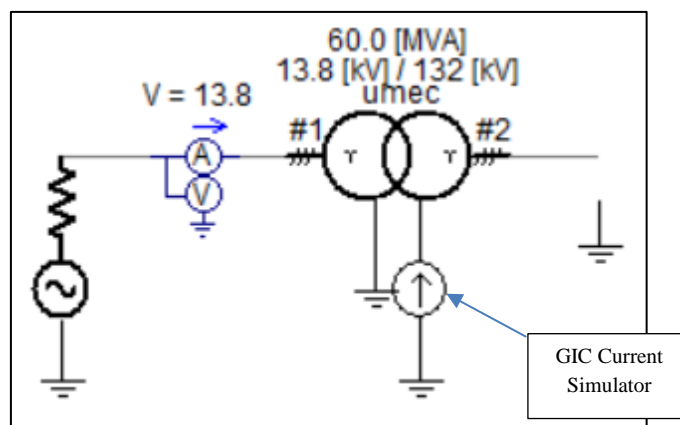


Figure 4.5, Model No.3 (PSCAD Model).

In PSCAD/EMTDC software package, there are two models of transformers. The first model is a general model where all basic transformer functions can be simulated assuming a linear magnetization characteristics, it is assumed that transformers do not saturate in system simulation. The second model is Unified Magnetic Equivalent Circuit (UMEC) Transformer Model. The UMEC model is a Norton equivalent model

derived directly from magnetic equivalent circuit analysis, where the saturation can be also simulated.

In GIC analysis, transformers part-cycle saturation is the major problem for the electric utility grid during GIC events, hence the transformer model used must be able to represent the electrical aspects of transformer saturation. The UMEC model is capable of simulating transformer saturation and hysteresis. The UMEC model allows configuration of I-V characteristic instead of the direct configuration of B-H characteristic directly.

CHAPTER 5

RESULTS AND DISCUSSIONS

5.1 Results

5.1.1 Model No.1 (Induction Model) Results

This model has been built using FEMM tool. The detailed structure of three-phase transformer core and windings have been generated in FEMM tool as described in Chapter 4. The main purpose of this FEM analysis is to simulate the exact shift of new operating flux density due to entering different GIC currents into HV winding transformer through its neutral points. The non-linear behavior of magnetic core has been defined in this model as shown in Figure 5.1, which is an actual data provided by core supplier of core grade M080-23P5-DR. The reluctance value is not a constant, it depends on the level of core saturation, and specifically on the magnitude of permeability.

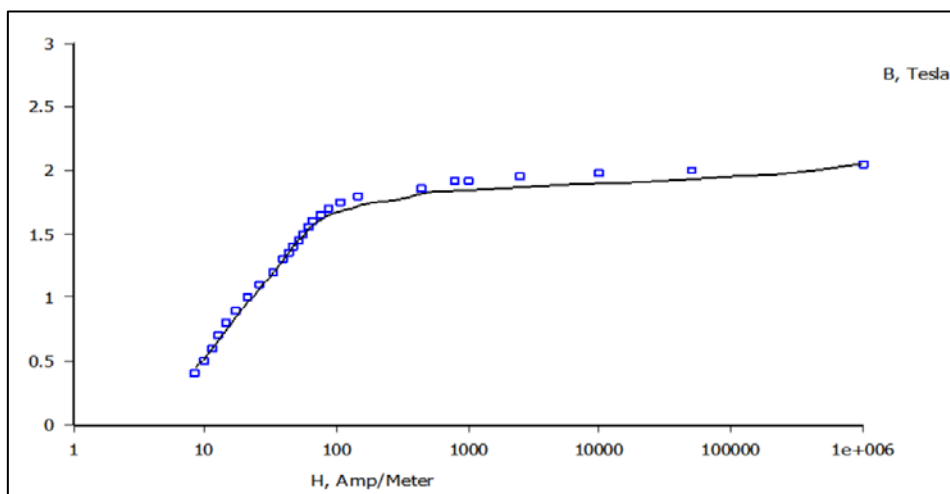


Figure 5.1, The defined BH curve in FEMM based on actual data collected from the core supplier.

The exact characteristics of core material have been defined in FEMM as illustrated in Figure 5.2. Non-linear material characteristics have been considered to simulate the core saturation. FEMM tool provides a possibility to define an accurate BH curve with a large number of points. The data of BH curve have been obtained from the core supplier, named Thessen Krupp core supplier from Germany [30].

To get an accurate DC shift of flux density at different GIC currents levels, a detailed structure of transformer active part (core and windings) enclosed by transformer tank border have been built using FEMM tool, as illustrated in previous Chapter 4.

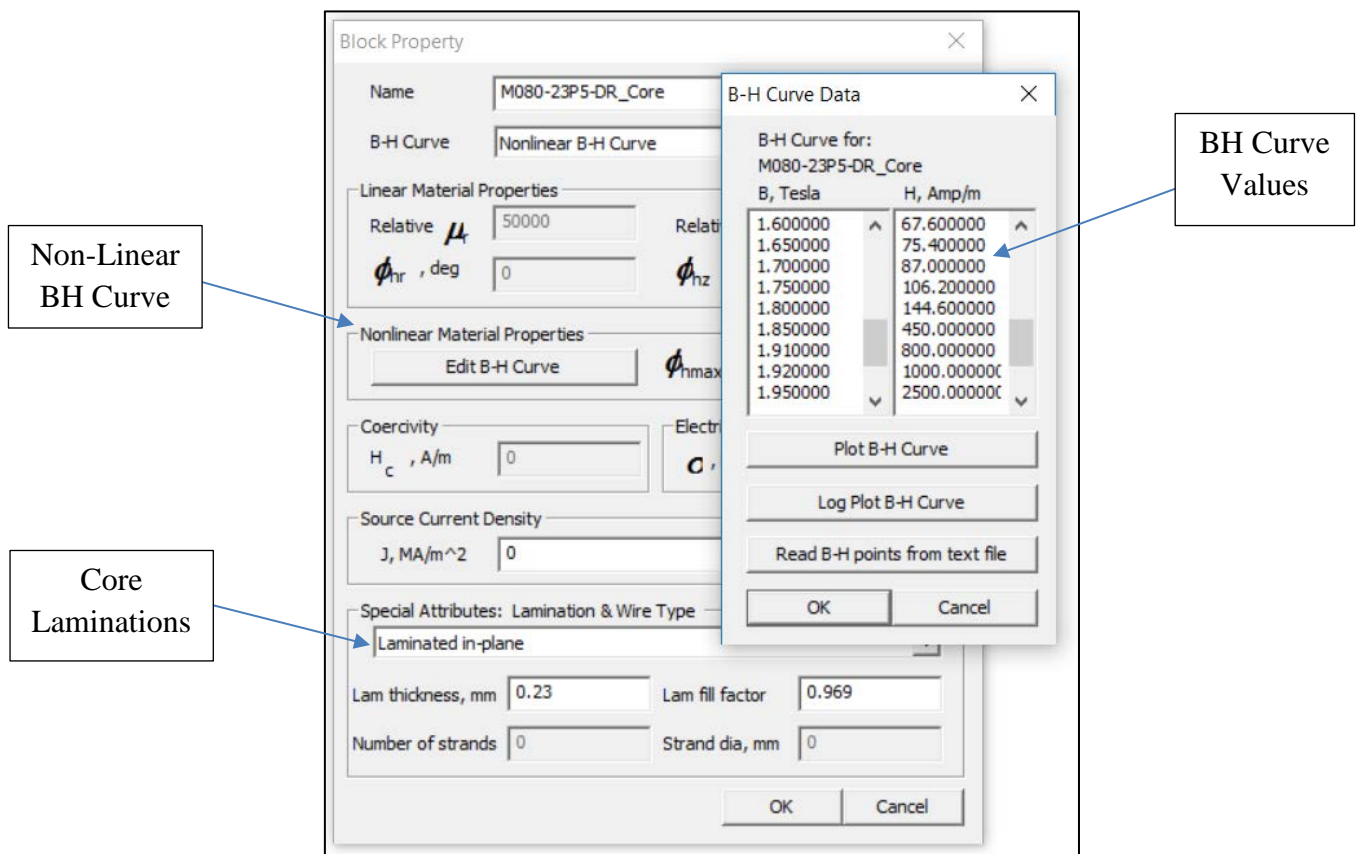


Figure 5.2, Defined core characteristics in FEMM tool.

The first step to evaluate the impact of GIC currents on power transformers is determining the new operating flux density, which is the sum of AC and DC fluxes.

Afterwards, the corresponding losses and noise are obtained using the well-known formulas described in Chapter 4.

The following cases have been simulated using Model No.1 (Induction Model), and utilizing FEMM tool. In each case DC shift in flux density is obtained using FEM analysis, the new operating flux density is then determined. The corresponding losses, temperature rise and noise are calculated:

- **Case No.1:** The no-load condition. The nominal flux density is considered to be ($B = 1.6$ T), with different GIC currents (50, 100, 150, 200, 250 and 300 A) is injected into transformer HV neutral point.

Figure 5.3 shows a normal operating condition at one instant of time, with zero GIC current. The current is zero in all windings except the LV winding, which carries the no-load current. The colored density plot is shown in right top corner and the exact operating flux density is shown in the output window in right bottom corner, which is 1.6 T.

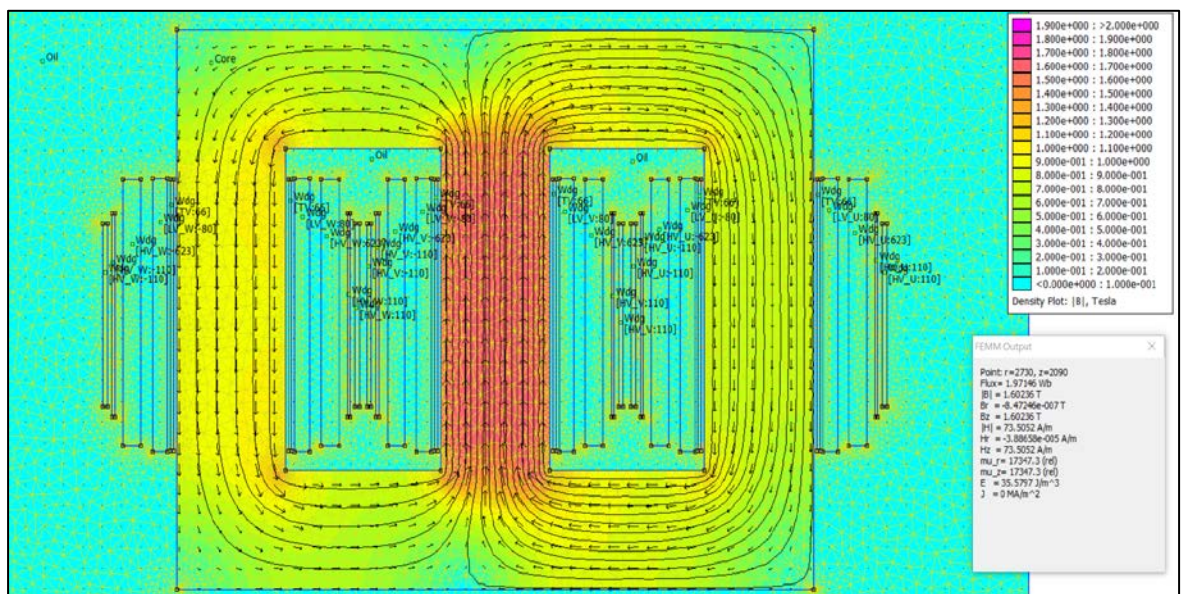


Figure 5.3, FEM induction model, normal condition with zero GIC current.

Table 5.1 shows the shift in flux density for various GIC currents from 50 A to 300 A. A GIC level of 50 A causes a magnetic flux density shift of 0.2889 T. The new operating flux density peak with 50 A GIC current is 1.8913 T. A GIC magnitude of 100 A increases the flux density shift by 0.0154 T, above what was caused by the 50 A GIC current. The next GIC currents steps of 150, 200, 250 and 300 A have only increased the flux density by only 0.0088, 0.0073, 0.0051 and 0.0049 T, respectively.

Table 5.1, Obtained flux density shift for different GIC levels, Case 1.

GIC Value (A)	$\Delta B(\text{DC})$ (T)	$B(\text{DC}+\text{AC})$ (T)
0	0.0000	1.6024
50	0.2889	1.8913
100	0.0154	1.9067
150	0.0088	1.9155
200	0.0073	1.9228
250	0.0051	1.9279
300	0.0049	1.9328

The increasing pattern of flux density shift reflects the non-linear nature of the core material. Higher values of GIC currents tend to drive the core deeper into saturation region. On the other hand, the permeability of core material significantly decreases, which limits the increase in flux density level. A 300 A GIC current failed to drive the core into 2.05 T, which represents the extreme saturation region.

In conclusion, we can say that very high level of GIC current is required to drive the core into full saturation region when the transformer is unloaded. Furthermore, the

higher GIC current steps cause less flux density shift, due to the significant reduction of permeability of core material in the saturation region.

The three limb core type power transformer is less sensitive to GIC current and more susceptible, due to the fact that no return core limb path exists to DC flux. The DC flux close the loop through a non-magnetic materials (tank wall, core clamps, and air).

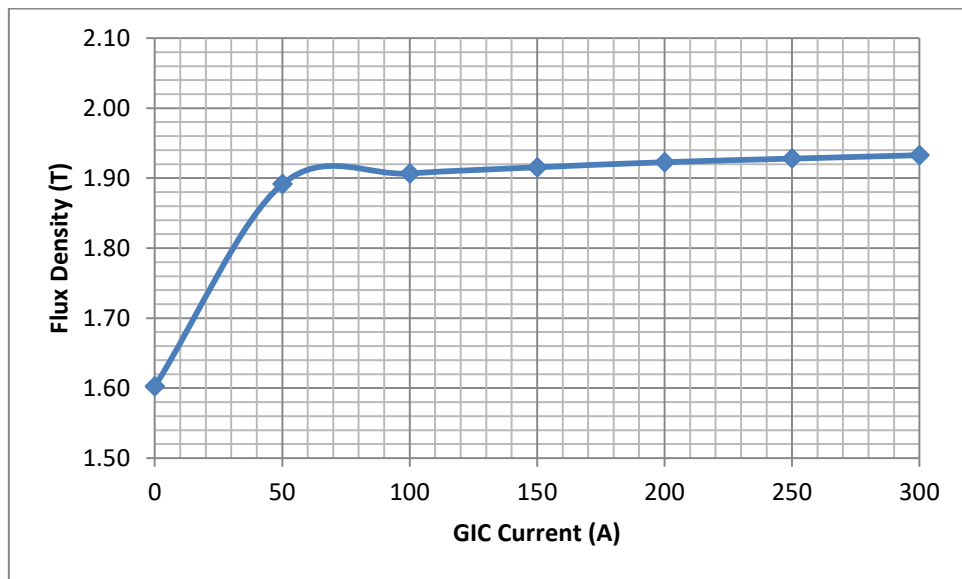


Figure 5.4, New operating flux density for different GIC levels.

The new operating flux density for different GIC values is shown in Figure 5.4. It is shown that the first step from 0 to 50 A is the highest one. Afterward much less variation occurred in flux density due to the non-linearity behavior of core.

Both core loss and noise level significantly increased by increasing GIC currents as shown in Table 5.2. An increase in core noise level is noticeable, which is a function of GIC level. Core losses might create a hot spot in the core and damage the insulation material which is in contact with the core (cooling channel and insulation pressboard).

Table 5.2, Core loss and noise level increase for different GIC levels.

GIC Value (A)	Core Loss (W)	Noise Level (dBA)
0	21,990	55.38
50	45,243	74.27
100	46,893	74.60
150	48,662	74.93
200	50,559	75.26
250	51,763	75.46
300	53,019	75.66

Due to the increase of core loss, the temperature of the core will experience a significant increase. The hot spot might be created within the core. However, core material can withstand temperatures in the range of 800°C (annealed temperature of core lamination during manufacturing), but the low temperature rise limit comes from the insulation of core laminations, pressboard insulation material (class A: 105°C) and core bolt insulation (class B: 130°C). Core surface and center temperatures rise are with the direct relationship with core losses as shown in Figure 5.5. Temperature rise limit for core usually is 120°C for the core surface temperature, and 140°C for the core hotspot (highest temperature in the core). The thermal time constant of the core, which is from 1 to 2 hours, plays a significant role in core's temperature rise. Assuming that GIC peaks are sustained for more than one hour, temperature rise values are obtained.

A significant increase in noise level is also noticed. The change is 18.89 dBA in the first step from 0 to 50 A GIC current. Afterward, less increase in noise level for 100 to 300 A GIC, due to less operating flux density shift.

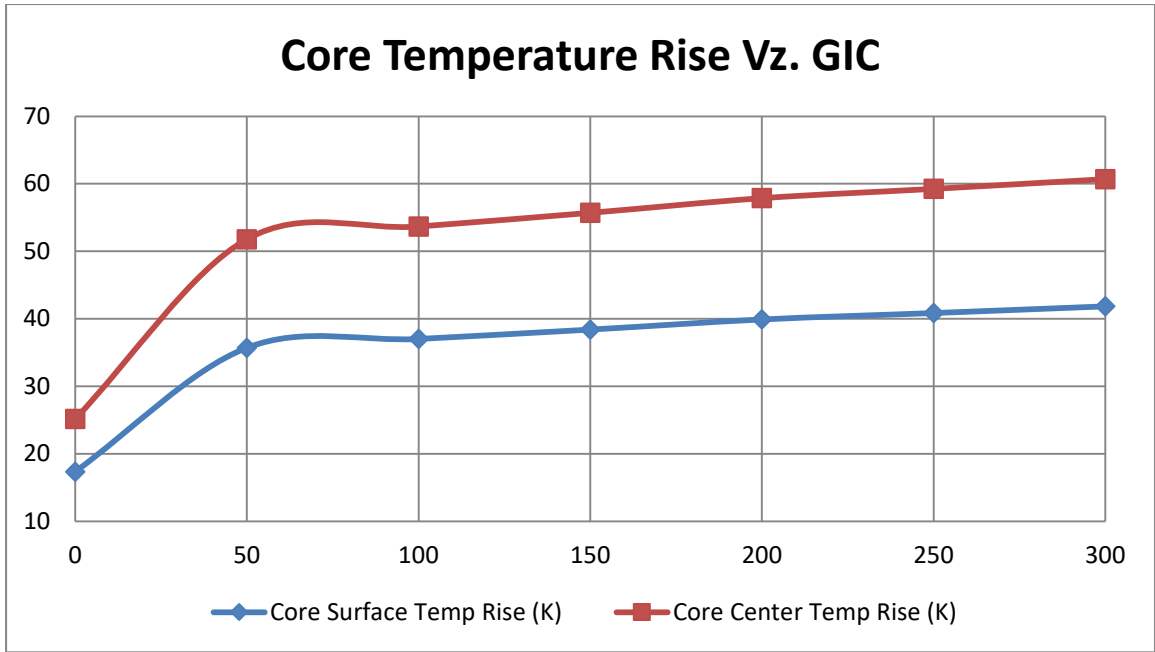


Figure 5.5, Core temperature rises at different GIC levels.

The maximum ambient temperature is 55 °C in Saudi Arabia. And the maximum guaranteed temperature rises are 45 K for top oil and 50 K for winding. Therefore the maximum allowed core temperature rise (surface) is 20 K, which is (20 K = 120 – 45 – 55).

- **Case No.2:** The no-load condition, with 90% of nominal flux density, with different GIC currents (50, 100, 150, 200, 250 and 300 A) are injected into transformer HV neutral point.

Table 5.3 shows the new operating flux density for different GIC current levels. Starting with a flux density of 1.4484 T, which is 90% of the nominal value. A GIC level of 50 A causes a magnetic flux density shift of 0.4427 T. The new operating flux density peak with 50 A GIC current is 1.8911 T. After that less changes of flux density in next GIC steps of 100 to 300 A.

Table 5.3, Obtained flux density shift for different GIC levels, Case 2.

GIC Value (A)	$\Delta B(\text{DC})$ (T)	$B(\text{DC}+\text{AC})$ (T)
0	0.0000	1.4484
50	0.4427	1.8911
100	0.0153	1.9064
150	0.0087	1.9151
200	0.0068	1.9219
250	0.0048	1.9267
300	0.0051	1.9318

It is observed that reducing the nominal flux density by 10% does not help against GIC phenomena. Due to a large number of HV winding turns, GIC current easily drives the core into saturation regardless of operation flux density. Hence to design transformer with low flux density level to survive against GIC phenomena is not an effective solution. It can be a solution for the regions where the GIC levels are with low levels, less than 10 A. In comparing with the original case (Case No.1) of operating flux density of 1.6 T. The same core loss, noise level and core temperature rises are obtained.

- **Case No.3:** The no-load condition, with upgraded core material type (M075-23PS-DR) and additional cooling duct in the transformer core. This case uses nominal flux density, and then injecting different GIC currents (50, 100, 150, 200, 250 and 300 A) into transformer HV neutral point.

Core loss and temperature rise are significantly reduced due to using upgraded core material and improved cooling system. This is achieved by adding one more cooling

channel. The core weight is increased by 200 kg to maintain the same operating flux density of 1.6 T.

Utilizing low loss core grade is a good solution to survive against GIC phenomena. Table 5.4 shows the advantage of utilizing better core grade of (M075-23PS-DR), which is the best core material type available in the market from losses point of view.

Table 5.4, Core loss and noise level increase for different GIC levels.

GIC Value (A)	Core Loss (W)	Noise Level (dBA)	Core Temperature Rise (K)
0	20,424	55.04	11.19
50	40,846	73.89	22.37
100	43,798	74.57	23.99
150	45,775	74.93	25.07
200	47,554	75.30	26.05
250	48,683	75.50	26.66
300	49,462	75.63	27.09

- **Case No. 4:** Simulate the DC shift with different GIC current with reduced HV winding turns, of course with increased volt per turn (Assumed 120% of the nominal volt per turn), and consequently larger core diameter to maintain same flux density.

Table 5.5 shows the new operating flux density for different GIC current levels, in case of reducing the number of turns of HV winding, with enlarged core diameter. It is observed that GIC level of 50 A causes a magnetic flux density shift of 0.2837 T. The new operating flux density peak with 50 A GIC current is 1.8861 T. The new operating flux densities are lower than Case No.1 and Case No.2, due to reduced number of turns of HV windings, which is the main driver of core saturation during GIC phenomena.

Table 5.5, Obtained flux density shift for different GIC levels, Case 5.

GIC Value (A)	$\Delta B(\text{DC})$ (T)	$B(\text{DC}+\text{AC})$ (T)
0	0.0000	1.6024
50	0.2837	1.8861
100	0.0138	1.8999
150	0.0094	1.9093
200	0.0046	1.9139
250	0.0045	1.9184
300	0.0029	1.9213

Redesigning the transformer with 120% of volt per turn (120.7 V/turn) will reduce the number of windings turns (Copper), and enlarge the core dimensions and weight. Table 5.6 summarizes the main parameters of the transformer with 120% volt per turn. Figure 5.6 shows the three different cases in one graph.

It is observed that transformer with less number of HV turns is more effective against GIC phenomena. The losses and temperature rise are lower in this case than Case No.1. However increasing volt per turn causes major changes in transformer, and might lead to non-optimized the transformer cost. 120% increase in volt per turn will directly increase the core weight.

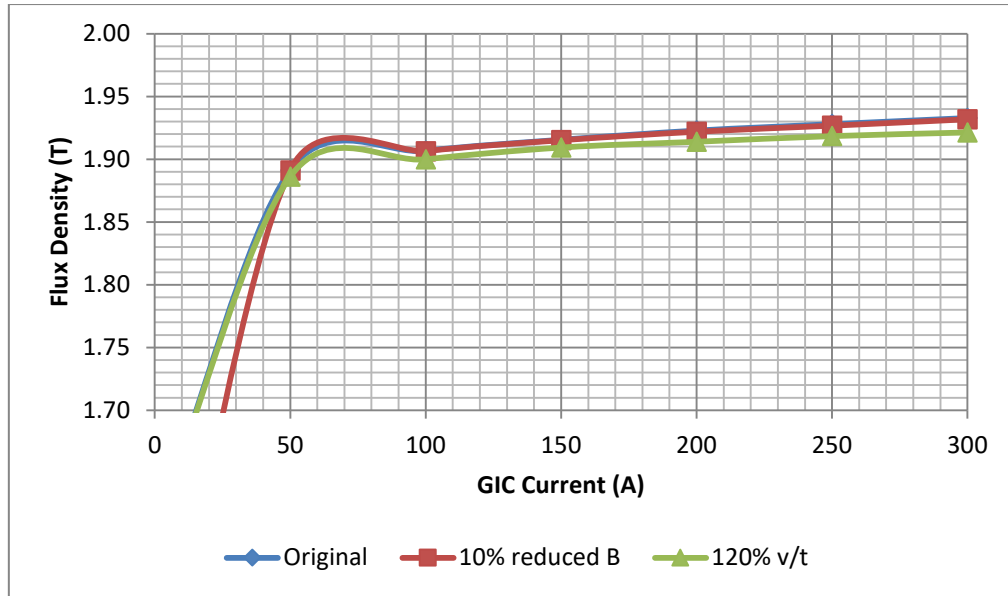


Figure 5.6, Three cases resulted flux density at different GIC level.

Table 5.6, Transformer main parameters with different volt per turn values.

Main Parameters	Volt per turn	
	99.59	120.7
LV Wdg Number of turns	80	66
HV Wdg Number of turns	843	694
Core Diameter (mm)	575	640
Core Weight (kg)	20213	25848
Copper Weight (kg)	11125	10091

5.1.2 Model No.2 (Stray Losses Model) Results.

The following cases of increased losses at different GIC values (0, 100, 200 and 300 A) have been simulated using FEMM tool:

- **Case No.1:** The full-load condition, with nominal operating conditions, with different GIC currents (100, 200 and 300 A) injecting into transformer HV neutral point.
- **Case No.2:** The overload condition (120% overload), with different GIC currents (0, 100, 200 and 300 A) injecting into transformer HV neutral point.

In each of above cases, the axial and radial flux densities components for each winding are obtained using FEM analysis. The corresponding eddy current losses are calculated using below equations. The eddy current loss is directly proportional to the squared of leakage flux components (axial and radial). Table 5.7 shows the results of Case No.1.

$$(Pe)_{axial} = \frac{\omega^2 B_y^2 t^2}{24\rho} \quad (5.1)$$

$$(Pe)_{radial} = \frac{\omega^2 B_x^2 w^2}{24\rho} \quad (5.2)$$

Where:

P : Eddy loss per unit volume.

B_x, B_y : Radial and axial flux densities components.

t, w : Thickness and width of conductor.

ρ : Resistivity.

Table 5.7, Transformer windings losses (resistive and stray) at different GIC levels, Case No.1.

		GIC Current (A)							
		0		100		200		300	
Winding	Component	Leakage (mT)	Loss (kW)	Leakage (mT)	Loss (kW)	Leakage (mT)	Loss (kW)	Leakage (mT)	Loss (kW)
TV	Radial	0.08	0.00	0.09	0.00	0.10	0.00	0.11	0.00
	Axial	57.02	1.57	44.54	0.96	31.52	0.48	18.45	0.16
	I2R		0.00		0.00		0.00		0.00
LV	Radial	0.30	2.49	0.34	3.18	0.38	3.95	0.45	5.35
	Axial	35.90	6.78	48.99	12.62	62.29	20.41	71.77	27.09
	I2R		109.98		111.15		111.55		111.86
HVM	Radial	0.25	2.02	0.23	1.69	0.21	1.37	0.18	1.08
	Axial	61.06	18.62	65.99	21.75	70.83	25.05	75.65	28.58
	I2R		81.58		105.97		133.54		164.29
HVC	Radial	0.44	0.36	0.50	0.46	0.56	0.58	0.62	0.71
	Axial	16.75	0.18	22.57	0.33	28.49	0.52	34.42	0.76
	I2R		18.49		23.01		0.00		0.00
HVF	Radial	0.35	2.28	0.40	2.95	0.45	3.70	0.50	4.54
	Axial	48.19	0.06	58.37	0.09	68.64	0.12	78.92	0.16
	I2R		19.57		0.00		0.00		0.00
Total Wdg Resistive Loss (kW)			229.62		240.13		245.09		276.16
Total Wdg Stray Loss (kW)			34.36		44.02		56.18		68.43
Total Transformer Wdg losses (kW)			263.98		284.15		301.26		344.59

The stray losses of normal condition (with zero GIC current) is 34.36 kW. After injecting 100 A of GIC current, the stray losses increased by 28% to be 44.02 kW. The resistive losses of windings also increased due to GIC current and additional magnetizing current by 4.5%. The leakage axial and radial flux densities are the integral of flux over each winding block over the block volume.

Magnetic leakage flux already exists outside core and between the windings in normal operating condition. It is represented by transformer reactance. But due to part-cycle saturation during the GIC phenomena, the leakage flux increased substantially and might create a hot-spot in transformer parts. There will be insignificant increase in core

and oil temperatures as their time constants are much larger values, in hours. Figure 5.7 illustrates the resulted leakage flux density for Case No.1 with 100 A GIC current.

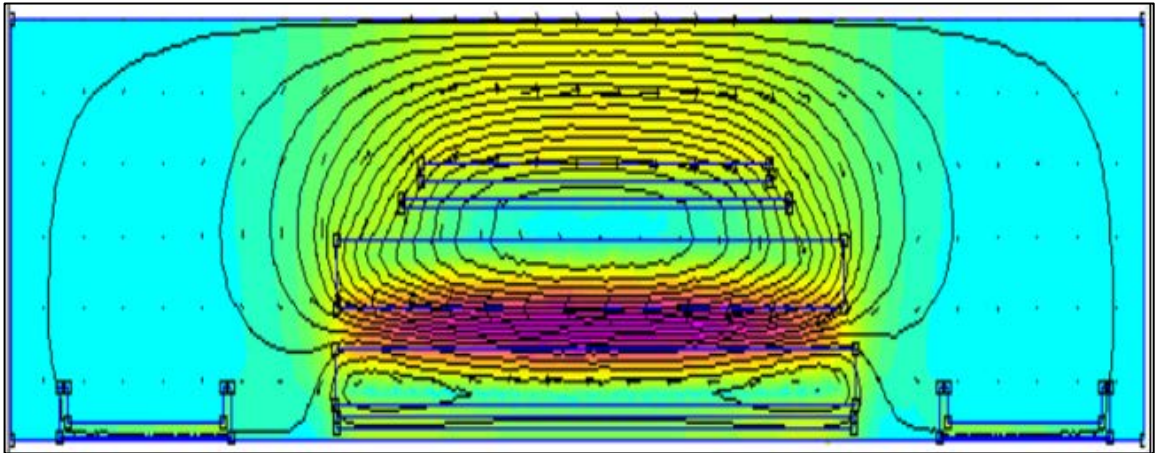


Figure 5.7, Leakage magnetic flux density in Case 1 with 100 A GIC.

Case No.2 results are summarized in Table 5.8, where 120% overloading condition have been considered. The leakage flux and stray losses increased in Case No. 2. Figure 5.8 illustrates the leakage flux density for Case No.2 with 100 A GIC current. In an overload condition, the flux density in core clamps exceeds 35 mT. But due to the large thermal time constant of mild steel, which is in hours, the temperature rise is limited.

Table 5.8, Transformer windings losses (resistive and stray) at different GIC levels, for Case No.2.

		GIC Current (A)							
		0		100		200		300	
Winding	Component	Leakage (mT)	Loss (kW)	Leakage (mT)	Loss (kW)	Leakage (mT)	Loss (kW)	Leakage (mT)	Loss (kW)
TV	Radial	0.10	0.00	0.11	0.00	0.12	0.00	0.13	0.00
	Axial	68.40	2.26	55.92	1.51	42.91	0.89	29.84	0.43
	I2R		0.00		0.00		0.00		0.00
LV	Radial	0.36	3.59	0.40	4.40	0.44	5.30	0.48	6.29
	Axial	43.09	9.77	56.18	16.60	69.48	25.39	82.80	36.06
	I2R		158.34		160.02		160.59		161.05
HVM	Radial	0.30	2.91	0.28	2.51	0.26	2.11	0.23	1.75
	Axial	73.27	22.34	78.20	25.45	83.03	28.70	87.86	32.13
	I2R		117.48		152.59		192.29		236.58
HVC	Radial	0.53	0.52	0.59	0.64	0.64	0.78	0.70	0.92
	Axial	20.10	0.26	25.92	0.43	31.84	0.65	37.77	0.92
	I2R		26.63		33.13		0.00		0.00
HVF	Radial	0.42	3.28	0.47	4.07	0.52	4.95	0.57	5.91
	Axial	57.83	0.09	68.01	0.12	78.28	0.16	88.56	0.20
	I2R		28.18		0.00		0.00		0.00
Total Wdg Resistive Loss (kW)			330.62		345.75		352.89		397.63
Total Wdg Stray Loss (kW)			45.01		55.74		68.93		84.61
Total Transformer Wdg losses (kW)			375.63		401.48		421.82		482.24

It can be observed that, in Case No.2 the leakage flux density significantly increased in the windings. Specifically, the radial leakage flux density on the top and bottom parts of the windings. It is also noticed that the magnitude of penetrated leakage flux density in the top and bottom core clamps increased. Which creates additional eddy current losses and might cause a hot spot in those location.

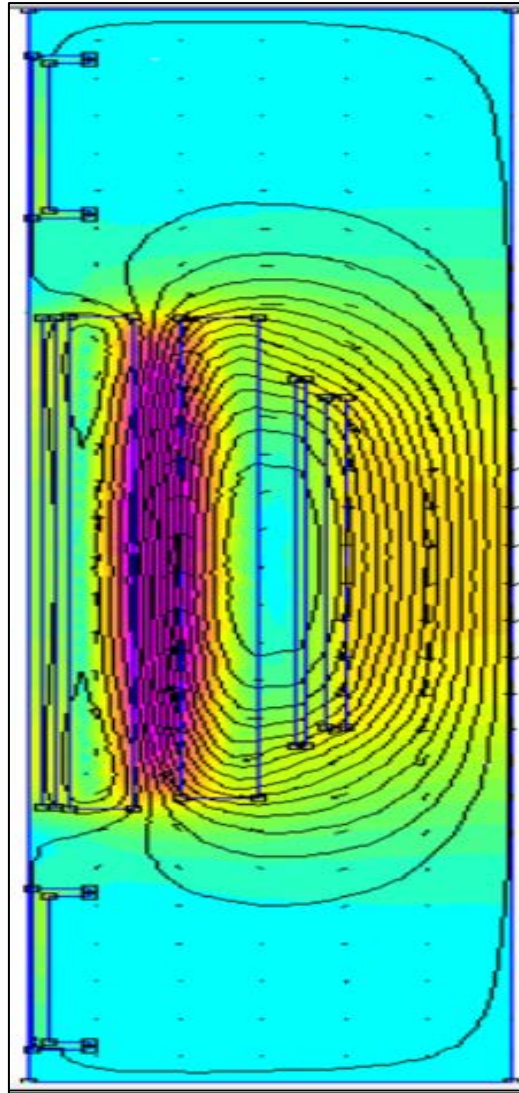


Figure 5.8, Leakage flux in Case 2 with 100 A GIC.

The windings temperature rise for Case No.1 and Case No.2 are tabulated in Table 5.9. In reference to equations (5.1) and (5.2) the stray losses of the windings can be minimized by subdividing the windings conductors into smaller strands.

Table 5.9, Winding temperature rise during different GIC level.

Case No.	Case 1				Case 2			
GIC Current (A)	0	100	200	300	0	100	200	300
Winding Temperature rise (K)	49.3	50.5	51.6	54.4	56.2	58.1	59.6	63.7

The eddy current loss due to the leakage magnetic field, which is produced by the load current and GIC phenomena, is calculated separately and then added to the resistive loss.

To reduce the resistive loss of copper conductor, the conductor dimensions are to be increased. In this way the eddy loss in windings increases. Hence, a compromise arrangement should be applied. The high values of radial or axial flux density can cause excessive loss and temperature rise.

The proper winding design is playing a significant role in improving the transformer losses and minimize the risk of hot spots creation, especially during the GIC events. In the absence of detailed FEM analysis, we used to take these limits to avoid excessive eddy loss, 12 to 14 mm conductor maximum width for 50 Hz and 10 to 12 mm maximum conductor width For 60 Hz frequency.

Subdividing the windings conductors into a number of parallel sub-conductors will reduce the eddy loss. It is directly proportional the squared of conductor dimensions. This is the most logical method of reducing eddy loss of windings. By subdividing the winding conductors or using bunched conductors of two or three parallel to enhance the space factor, the conductor fabrication price will be increased. Furthermore, the short-circuit withstand consideration of conductor dimensions should be also taken into consideration while designing.

A continuously transposed conductor (CTC), where a number of small strand rectangular conductors are used in one cable and continuously transposed at regular intervals. In CTC, the conductor thickness can reach to 1.2 mm and width of 3.8 mm, resulting in less amount of eddy current loss. The high cost of CTC should be

compensated by the advantage gained by the reduction of losses. The fabrication cost of CTC varies with conductor dimensions and the number of strands.

Two different conductors' widths can be used along the winding height. Smaller conductor width to be used at the windings end, where the radial flux density component is the dominant and incident perpendicularly on the conductors width as observed by FEM analysis. The top and bottom end discs of HV winding might be designed with less number of turns per disc, with larger thickness and lower width.

A combination of above solutions has been simulated in this thesis. Where a mix of rectangular bunched conductors and CTC conductors are used at the top and bottom of winding to minimize the eddy loss. The CTC conductor is used for a few top and bottom discs instead of using CTC overall the winding height. In this case, the cost is more optimized instead of using CTC overall the winding height.

5.1.3 Model No.3 (PSCAD Model) Results.

PSCAD model will be mainly used to simulate the behavior of transformer during different GIC levels, which will be injected through its grounded neutral. VAR consumption, current waveform of magnetization current will be studied at different GIC levels.

In PSCAD/EMTDC software package, two models of the transformer are available, a general model and a special model. The general model will not help us in our study, as it assumes that transformers do not saturate and linear magnetization characteristics are considered. The model is not suitable for this application of GIC modeling. The special model referred to Unified Magnetic Equivalent Circuit Transformer Model (UMEC). The magnetization curve of the transformer core and all transformer parameters are defined by the user. The saturation phenomena can be simulated.

The UMEC model is capable of simulating transformer saturation and hysteresis. The UMEC model allows configuration of I-V characteristic instead of the direct configuration of B-H characteristic directly.

In order to investigate the relationship between reactive power losses and GIC magnitude, 60 MVA, 132/13.8 kV three-limb power transformer main parameters have been defined in UMEC transformer model in PSCAD as shown in Figure 5.9. The I-V magnetization characteristic is shown in Figure 5.10.

Configuration	
Transformer name	T1
Transformer core construction	Three-limb
Transformer MVA	60.0 [MVA]
Primary voltage (Line-Line, RMS)	13.8 [kV]
Secondary voltage (Line-Line, RMS)	132 [kV]
Winding #1 Type	Y
Winding #2 Type	Y
Delta lags or leads Y	Lags
Base operation frequency	60.0 [Hz]
Leakage reactance	0.22 [pu]
No load losses	0.001 [pu]
Copper losses	0.04 [pu]
Model saturation?	Yes
Tap changer winding	None
Graphics Display	Single line (circles)
Display Details?	Yes

Figure 5.9, Main transformer parameters defined in PSCAD.

Saturation Curve	
Magnetizing current at rated voltage	1 [%]
Enable Saturation	1
Point 1 - Current as a % of rated current	0.0 [%]
Point 1 - Voltage in pu	0.0 [pu]
Point 2 - (I , V)	.1774 [%] .324129 [pu]
Point 3 - (I , V)	.487637 [%] .61284 [pu]
Point 4 - (I , V)	.980856 [%] .825118 [pu]
Point 5 - (I , V)	2 [%] 1 [pu]
Point 6 - (I , V)	3.09543 [%] 1.08024 [pu]
Point 7 - (I , V)	6.52348 [%] 1.17334 [pu]
Point 8 - (I , V)	20.357 [%] 1.26115 [pu]
Point 9 - (I , V)	60.215 [%] 1.36094 [pu]
Point 10 - (I , V)	124.388 [%] 1.49469 [pu]

Figure 5.10, Defined saturation curve parameters in PSCAD.

The obtained magnetization current curve with zero GIC current is shown in Figure 5.11, where a peaky shape of the waveform is shown. And no shift in magnetizing current is noticed.

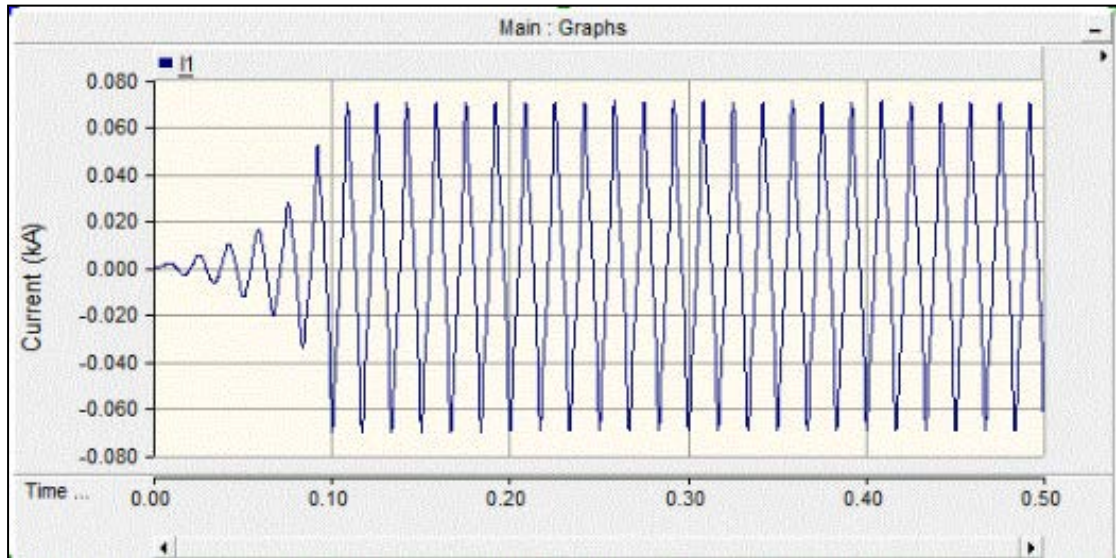


Figure 5.11, Magnetization current waveform with zero GIC current.

Figure 5.12 and Figure 5.13 show the magnetization current waveforms with 50 A and 100 A GIC current. The magnetization current waveforms have been shifted due to driving the core into saturation. The shape of current has not been affected due to the fact that PSCAD saturation curve is defined as a linear piece-wise function, interconnecting the determined 10-points of I-V in PSCAD.

A linear relationship between the increased GIC current and reactive power consumption of transformer is obtained for different GIC currents. Figure 5.14 shows the obtained linear relationship, which agrees with obtained results in [1].

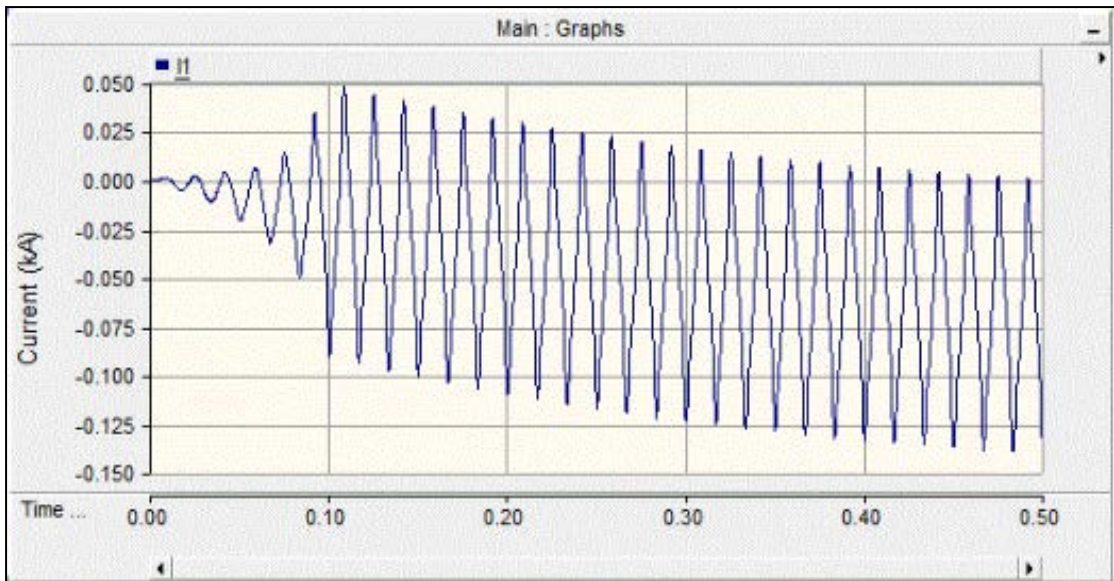


Figure 5.12, Magnetization current waveform with 50 A GIC current.

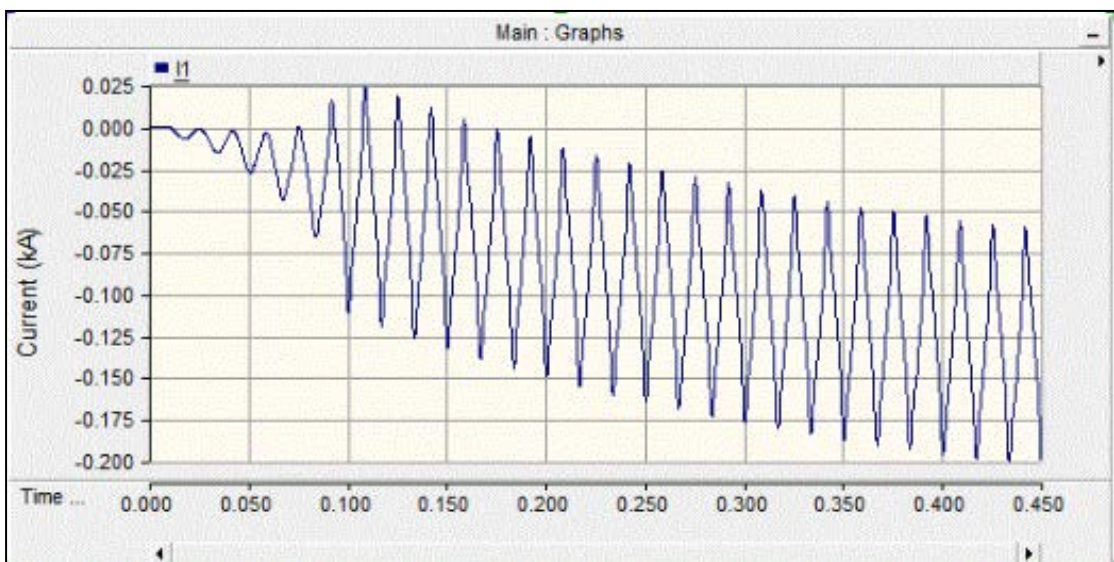


Figure 5.13, Magnetization current waveform with 100 A GIC current.

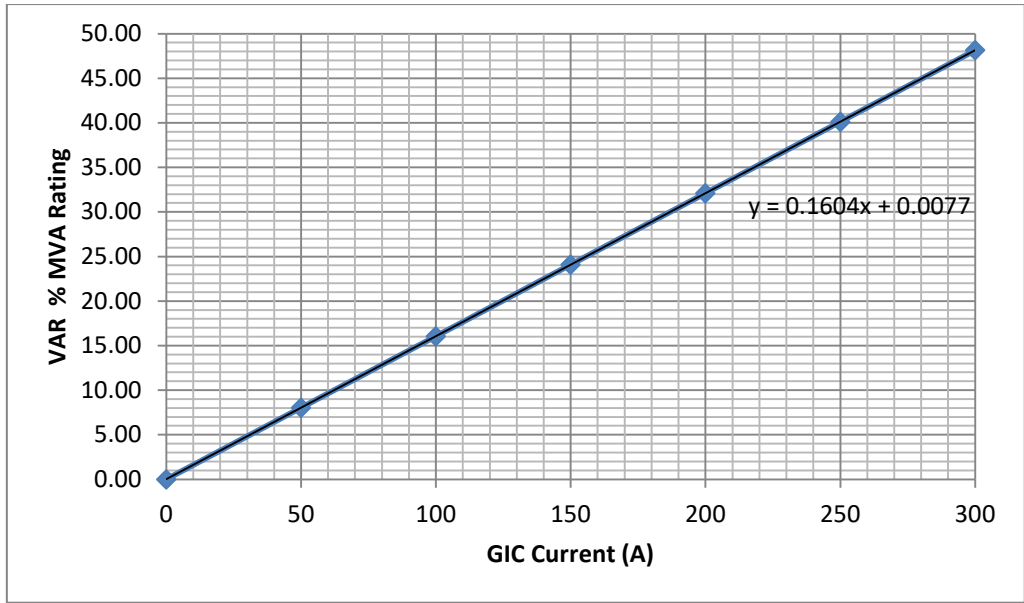


Figure 5.14, A linear relationship between GIC and reactive power consumption.

5.2 New Transformer Design.

This section presents a modified transformer design to alleviate the problems likely to be faced by the flow of the GIC currents. The design adopts several techniques.

I. Upgrade transformer core material (low loss grade).

The original design is using core material of grade M080-23P5-DR. The proposed core material is M075-23P5-DR, which has lower loss value. Table 5.10 gives the main characteristics of those different core materials grades.

Table 5.10, Core materials characteristics.

Core Materials Grade	Nominal thickness (mm)	Specific total loss at 1.7 T, 60 Hz (W/kg)		Magnetic Polarization for H = 800 A/m (T)	Density (kg/m ³)
		Maximum	Typical		
M115-27S5	0.27	1.50	1.45	1.83	7650
M075-23P5-DR	0.23	1.00	0.97	1.91	7650
M080-23P5-DR	0.23	1.06	1.04	1.91	7650

M115-27S5 is the most common used material in power transformer. It has higher losses and lower saturation level compared with M085-23P5-DR and M075-23P5-DR. M075-23P5-DR core material is very low loss material, it is considered as the best material currently available in the market. The availability of this material is not always guaranteed, it is usually used only for particular cases with very high loss capitalization and it is the proposed grade in case of GIC.

Table 5.11 shows the core grade cost rate (\$/kg) in the market as of quarter four 2017. M075-23P5-DR is more expensive than M085-23P5-DR by around 0.4 \$/kg (14.5% higher cost of the same core) [34].

Table 5.11, Core materials costing rate, as of Q4-2017.

Core Materials Grade	Costing Rate (\$/kg)
M115-27S5	2.6
M075-23P5-DR	3.2
M080-23P5-DR	2.8

Using M075-23P5-DR, the core loss is reduced by 7% at nominal induction level (from 21.9 kW to 20.4 kW). At 50 A GIC current the core loss reduced also by 7%. Accordingly, the core temperature rise also reduced by 1.62 K at 50 A GIC case.

II. Adding additional cooling channel to the core.

Another approach is to add an additional cooling duct and to increase the core diameter from 575 mm to 580 mm. By adding an additional cooling duct to the core, and increasing core diameter from 575 mm to 580 mm to maintain the same operating flux density, the cooling efficiency will be increased. An additional cooling duct of 6 mm has enhanced the cooling results, by allowing the oil to flow through the middle of the core. The core temperature rise reduced at 50 A GIC case from 35.7 K to 23.99 K, with an increase in core weight by 113 kg (from 20197 kg to 20310 kg).

III. Using of upgraded insulation material wherein contact with the core.

The core material can withstand temperatures in the range of 800°C (annealed temperature of core lamination during manufacturing). The temperature rise limit is decided by the insulation of core laminations, pressboard insulation (class A: 105°C) and core bolt insulation (class B: 130°C) that might get damaged.

High-temperature insulation materials, like Nomex material, to be used instead of class A materials in the core. However the thermal time constant of the steel material is in hours, but to guarantee that no insulation damage might occur to core during sever GIC phenomena.

IV. Reduce the number of HV winding turns by increasing volt per turn parameter of the transformer.

The number of HV winding is one the main deciding factor of flux density shift during GIC phenomena. The GIC current multiplied by number turn of HV winding represents the DC magnetomotive force (MMF) that drives the core into saturation. A reduction in the number of HV winding turns number will significantly decrease the magnitude of DC shift of flux density. To do so and to maintain the same voltage level of windings, volt per turn parameter should be increased with the same percentage. Increasing volt per turn value with the same operating flux density requires larger core cross-sectional area. Consequently, the core weight will be increased, but the copper weight also will be reduced.

By reducing number of HV turns from 843 to 694. The core diameter increased from 575 mm to 640 mm and accordingly the core weight increased by around 5.5 ton. The copper weight reduced by around one ton. The saving in reducing the copper weight is

2.5 times the cost of the increasing the core weight. Increased volt per turn will cause major changes in the transformer, and might lead to non-optimized transformer cost. On the other hand, it reduces the magnetic flux density shift during GIC phenomena as shown in Table 5.5.

V. Change of HV winding conductor design, top and bottom parts.

As observed by a detailed FEM analysis the main radial leakage flux density is on the top and bottom parts of windings, where the axial conductor dimension is the main deciding factor of stray losses. To minimize the hot spot values in the top and bottom of HV winding, one of the followings solutions can be utilized.

Subdividing the windings conductors into a number of parallel sub-conductors will reduce the eddy loss. It is directly proportional the squared of conductor dimensions. This is the most logical method of reducing eddy loss of windings. By subdividing the winding conductors or using bunched conductors of two or three parallel to enhance the space factor, the conductor fabrication price will be increased. Furthermore, the short-circuit withstand consideration of conductor dimensions should be also taken into consideration while designing.

A continuously transposed conductor (CTC), where a number of small strand rectangular conductors are used in one cable and continuously transposed at regular intervals. In CTC, the conductor thickness can reach to 1.2 mm and width of 3.8 mm, resulting in less amount of eddy current loss. The high cost of CTC should be compensated by the advantage gained by the reduction of losses. The fabrication cost of CTC varies with conductor dimensions and the number of strands.

Two different conductors' widths can be used along the winding height. Smaller conductor width to be used at the windings end, where the radial flux density component is the dominant and incident perpendicularly on the conductors' width as observed by FEM analysis. The top and bottom end discs of HV winding might be designed with less number of turns per disc, with larger thickness and lower width.

A combination of above solutions has been simulated in this thesis. Where a mix of rectangular bunched conductors and CTC conductors are used at the top and bottom of winding to minimize the eddy loss. The CTC conductor is used for a few top and bottom discs instead of using CTC overall the winding height. In this case, the cost is more optimized instead of using CTC overall the winding height.

The proposed design will decide the type of conductors in 92 HV winding discs. The top part consists of 18 discs of CTC, bottom part also with 18 disc with CTC and the remaining 56 discs left as per original design with the rectangular conductor. The new CTC conductor is with 15 rectangular strands, each strand with 4.4 mm by 1.4 mm dimension. The original design conductor width is 9 mm.

Table 5.12 shows the effect of changing 40% of HV winding by CTC conductor. The stray losses are reduced by 35% at zero GIC to 43% at 300 A GIC. On the other hand, the winding cost increased by the difference between the fabrications costs of bunched rectangular conductor and CTC conductor. The fabrication cost of the bunched rectangular conductor is 1.7 \$/kg, where the CTC fabrication cost is 2.1 \$/kg. Hence the overall increased winding cost will be 9.5% as only 40% of winding height is modified.

Table 5.12, Transformer windings losses at different GIC levels, for Case No.1, with CTC.

		GIC Current (A)							
		0		100		200		300	
Winding	Component	Leakage (mT)	Loss (kW)	Leakage (mT)	Loss (kW)	Leakage (mT)	Loss (kW)	Leakage (mT)	Loss (kW)
TV	Radial	0.08	0.00	0.09	0.00	0.10	0.00	0.11	0.00
	Axial	57.02	1.57	44.54	0.96	31.52	0.48	18.45	0.16
	I2R		0.00		0.00		0.00		0.00
LV	Radial	0.30	2.49	0.34	3.18	0.38	3.95	0.45	5.35
	Axial	35.90	6.78	48.99	12.62	62.29	20.41	71.77	27.09
	I2R		109.98		111.15		111.55		111.86
HVM	Radial	0.25	2.02	0.23	1.69	0.21	1.37	0.18	1.08
	Axial	61.06	8.70	65.99	10.16	70.83	11.71	75.65	13.36
	I2R		81.58		105.97		133.54		164.29
HVC	Radial	0.44	0.36	0.50	0.46	0.56	0.58	0.62	0.71
	Axial	16.75	0.08	22.57	0.15	28.49	0.24	34.42	0.36
	I2R		18.49		23.01		0.00		0.00
HVF	Radial	0.35	2.28	0.40	2.95	0.45	3.70	0.50	4.54
	Axial	48.19	0.06	58.37	0.09	68.64	0.12	78.92	0.16
	I2R		19.57		0.00		0.00		0.00
Total Wdg Resistive Loss (kW)			229.62		240.13		245.09		276.16
Total Wdg Stray Loss (kW)			24.35		32.26		42.56		52.80
Total Transformer Wdg losses (kW)			253.97		272.39		287.64		328.95

Table 5.13 shows the winding temperature rise in improved Case No.1. The guaranteed winding temperature rise of this transformer is 50 K, hence utilizing CTC conductor on top and bottom parts of HV winding has led to withstand of GIC current of 100 A.

Table 5.13, Winding temperature rise in improved Case No.1 during different GIC level.

Case No.	Improved Case 1			
GIC Current (A)	0	100	200	300
Winding Temperature rise (K)	48.6	49.4	50.7	52.9

VI. Adding magnetic shunt on top and bottom of core yoke clamps in addition to tank walls.

As found by FEM analysis, the magnitude of flux density in the top and bottom core yoke clamps are increased and might cause a hot spot rise at those locations. However the thermal time constant of steel is in hours. To avoid hotspot creation, a magnetic shunt is highly recommended to be installed at those locations. Magnetic shunt materials is the same as silicon steel core material with very low losses compared with mild steel characteristics. The stray losses will be significantly reduced.

VII. Inserting non-magnetic steel parts in transformer tank and core clamps.

Inserting non-magnetic materials into the steel structure and core clamps will significantly reduce the permeability and accordingly increasing the reluctance value of the leakage flux path. In such a way the magnetic flux density shift during GIC phenomena will be also smaller and the stray losses will be much less. This case is not simulated in this thesis.

Figure 5.15 shows the flow chart of the adopting mechanism of new design techniques to improve the transformer withstand ability against GIC phenomena or any DC excitation source.

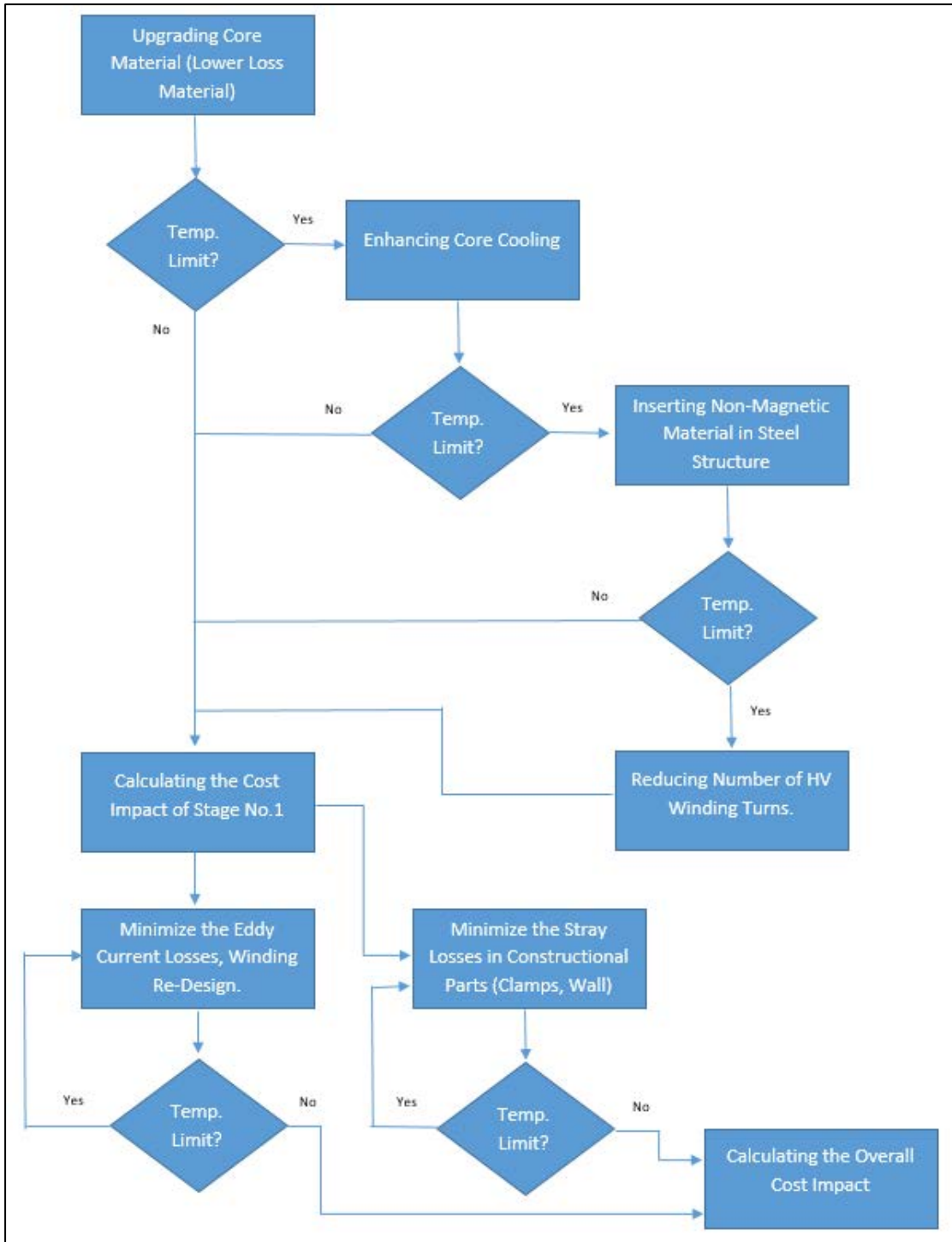


Figure 5.15, Flow chart of the adopting mechanism of new design techniques.

5.3 Cost-benefit Analysis

In addition to the benefits gained by utilizing some of the mentioned improved design techniques to strengthen the transformer against GIC phenomena, the power transformer cost will be affected due to the cost impact of each enhancement case. The following sections highlight the cost impact of each technique beside its added benefits. It was expected from the beginning of this project that an additional cost will appear in the transformer to improve its capability to survive against GIC phenomena, however, such increase will extend the life of transformer and avoid any interruption in electric power supply during sever GIC phenomena.

Upgrading the core material grade from M080-23P5-DR to M075-23P5-DR, which has a lower specific loss value (Watt/kg). The core loss reduced by 7% at nominal induction and at 50 A GIC case. The core temperature rise also reduced by 1.62 K at 50 A GIC case. On the other hand, the core cost increased by 14.5% due to utilizing more expensive core material.

Enhancing the cooling efficiency of core by adding one more additional cooling duct at the middle of the core has led to a significant reduction in core temperature rise. For 50 A GIC case, the core temperature rise reduced from 35.7 K to 23.99 K. Due to this reduction in temperature rise, it can be said that transformer can withstand 50 A GIC without any major insulation damage, especially core insulation materials. On the other hand, the core diameter increased to maintain the same operating flux density, from 575 mm to 580 mm. Enlarging the core diameter increased the core weight from 20197 kg to 20310 kg. And consequently, the core cost increased by 0.6%.

Utilizing the high-temperature insulation materials for core will also have a major cost impact. Nomex materials can withstand much higher temperature level than Class A or Class B materials. It has also higher cost, which is around double of the price. In case of using high loss core grade material, it is highly recommended to go with such high-temperature material to avoid any insulation damage, which might lead to transformer failure.

Copper and core weights are always compromised during transformer design stage to achieve the optimal cost design. Designing the transformer with higher volt per turn value will enlarge the core and reduce the copper weights. This might lead to non-optimal design. Higher volt per turn means lower number of windings turns, which means lower DC magnetomotive force (MMF) during GIC.

Referring to Case No.4 of induction model, HV winding turns number reduced from 843 to 694. The core diameter increased from 575 mm to 640 mm and accordingly the core weight increased by around 5.5 ton. The copper weight reduced by around one ton. The copper LME (London Metal Exchange) value is 6.7 \$/kg, whereas the core rate is around 3 \$/kg as of quarter four 2017. A fabrication cost of 2 \$/kg is always added to the copper cost, so in total copper cost is 8.7 \$/kg and core cost is 3 \$/kg.

Hence the overall transformer cost will be increased by $\{(5,500 \text{ kg} \times 3 \text{ $/kg}) - (1,000 \text{ kg} \times 8.7 \text{ $/kg}) = 7,800 \text{ \$}\}$. It represents 5% of copper and core cost.

Windings stray losses can be reduced by proper selection of windings conductor's dimensions. However, conductor's dimensions are usually determined to meet a certain guaranteed resistive loss and impedance value. The radial magnetic leakage flux is dominant at the top and bottom parts of the windings as observed by detailed FEM analysis.

The new windings conductors design has led to reducing stray losses by 35% with zero GIC to 43% in 300 GIC current case. A combination of rectangular conductor and CTC conductors are used at the top and bottom of winding (40% of winding height) to minimize the eddy loss. The CTC conductor is used for a few top and bottom discs instead of using CTC overall the winding height.

Changing the conductor's type and dimensions led to increasing winding cost. The fabrication costs of bunched rectangular conductor and CTC conductor are 1.7 \$/kg and 2.1 \$/kg, respectively. As only 40% of HV winding conductor type changed, the winding cost increased by 9.5%. On the other hand, the winding temperature rise for 100 A GIC case will be below the guaranteed temperature rise $49.4 \text{ K} < 50 \text{ K}$. Table 5.14 summarizes the main new transformer design the cost-benefits analysis.

Table 5.14, Summarized cost-benefits analysis of new transformer design.

Item No.	Adopted Technique	Gained Benefits	Cost Impact
1	Upgrading the core material grade from M080-23P5-DR to M075-23P5-DR.	The core loss reduced by 7%. The core temperature rise reduced by 1.62 K at 50 A GIC case.	The core cost increased by 14.5%.
2	Enhancing the cooling efficiency of core by adding one more additional cooling duct at the middle of the core.	The core temperature rise reduced from 35.7 K to 23.99 K, in 50 A GIC case.	Core Weight increased by 113 kg. The overall core cost increased.
3	Utilizing the high temperature insulation materials for core (Nomex).	Withstand much higher temperature level than Class A or Class B materials.	Core insulation cost is doubled.
4	Designing the transformer with higher volt per turn value.	HV winding turns number reduced from 843 to 694. Lower MMF and DC flux shift during GIC. The copper weight reduced by one ton.	The core weight increased by 5.5 ton. Overall transformer cost increased by 5%.
5	Redesigning of the top and bottom windings parts.	Reduction in stray losses by 35% with zero GIC to 43% in 300 GIC case. Winding temperature rise for 100 A GIC is 49.4 K, lower than 50 K.	The winding cost increased by 9.5%.
6	Adding magnetic shunt on top and bottom of core yoke clamps.	To avoid any hot spot creation at those locations due to exceeding 35 mT limit flux density.	Core Clamp cost increased due to adding the shunt. 5% max.
7	Inserting non-magnetic steel parts in transformer tank.	To increase the Reluctance path of return leakage flux. And get lower DC shift.	Tank fabrication might increase by 5 to 10% max.

The overall cost increase in the new power transformer that can survive against 100 A GIC current is 9%. It was expected from the beginning of this project that an additional cost will appear in transformer to improve its capability to survive against GIC phenomena, however such increase will extend the life of transformer and avoid any interruption in electric power supply during sever GIC phenomena.

Table 5.15, Percentage increase of new design cost.

Transformer Main Component	Cost Percentage out of Total Transformer Cost	Increased by	Contribution on Overall Transformer Cost
Copper	30%	10%	2.85%
Core	20%	20%	4.00%
Steel Structure	20%	10%	2.00%
Oil	6%	0%	0.00%
Insulation	5%	0%	0.00%
Accessories	19%	0%	0.00%
Total			9%

CHAPTER 6

CONCLUSIONS AND FUTURE WORK

6.1 Conclusions

Thesis findings and conclusions can be summarized as follows:

- A comprehensive literature review has been accomplished on the main reported GIC events worldwide since 1989 till today. Investigating the main affected transformer parts and performance.
- The effects of different GIC events on power transformers have been thoroughly evaluated under different operating conditions, no-load and loaded conditions.
- Detailed FEM simulation of power transformers behavior during the GIC phenomena. Two detailed FEM models have been created to simulate the power transformer behavior when subjected to such a phenomena. The first model is to find out an accurate induction shift due to GIC current, and the second model is to evaluate the additional stray losses that might occur in windings.
- Modeling of power transformer response to the GIC phenomena using a PSCAD tool. The saturation behavior of power transformer has been

modeled using the PSCAD to exactly find out the relationship between GIC levels and absorbed reactive power, which is a linear relationship.

- Using the FEM tool to evaluate the eddy current losses in windings, by finding out the exact leakage flux components (axial and radial) and to control it by redesigning the winding parts where the radial leakage flux densities are dominant.
- Specify the main locations in power transformer where magnetic shunts should be added in parallel with steel structure parts to avoid any hotspot creation (Tank Wall, Core Clamps), Based on FEM analysis of magnetic leakage flux distribution.
- Proposed different design techniques that reduce the severity of GIC event along with their cost impact, such that core material and design, windings type and design, utilizing non-magnetic materials in tank structure.
- Conducting the cost-benefits analysis on all proposed design techniques that enhance the withstand ability level of power transformer against GIC event. To withstand 50 A GIC current without any trouble, 15.1% increase in core cost, 5% increase due to higher volt per turn and 9.5% increase to account for the change in windings type and design. Those increased costs in each part have strengthened the transformer to withstand 50 A GIC current.

6.2 Recommendations for Future Work

- To use 3D model instead of 2D model to obtain more accurate results.
- To evaluate the GIC effects on higher voltage class power transformer, 500 kV or higher.
- To simulate the transformer behavior under GIC event in presence of different abnormal conditions like transient and short circuit events.

References

- [1] Transformers Committee of the IEEE Power and Energy Society, "C57.163-2015-IEEE Guide for Establishing Power Transformer Capability while under Geomagnetic Disturbances" IEEE Power and Energy Society, New York, NY 10016-5997, 2015.
- [2] Philip R. Price, "Geomagnetically Induced Current Effects on Transformers" IEEE Transaction on Power Delivery, Vol. 17, No. 4, October 2002.
- [3] Girgis, R., and K. Vedante, "Methodology for Evaluating the Impact of GIC and GIC Capability of Power Transformer Designs" IEEE Power & Energy Society 2013 General Meeting Proceedings, Vancouver, Canada, pp. 1–5, July 2013.
- [4] Girgis, R., and K. Vedante, "Effect of GIC on Power Transformers and Power Systems" IEEE Transmission and Distribution Conference, Orlando, FL, May, 2012.
- [5] R. Girgis, K. Vedante and K. Gramm "Effects of Geomagnetically Induced Currents on Power Transformers and Power Systems" CIGRE Paper #A2-304, August 2012.
- [6] T. Ngnegueu, F. Marketos, F. Devaux, R. Bardsley, S. Barker, "Behavior of Transformers under DC/GIC Excitation: Phenomenon, Impact on Design/Design Evaluation, Process and Modeling Aspects in Support of Design," CIGRE Paper # A2–303, 21, rue d'Artois, F-75008 Paris, August 2012.
- [7] B. Zhang, L. Liu, Y. Liu, M. McVey, R.M. Gardner, "Effect of geomagnetically induced current on the loss of transformer tank" Published in IET Electric Power Applications, IET Electr. Power Appl., 2010, Vol. 4, Iss. 5, pp. 373–379, 2009.
- [8] R. Nishiura, S. Yamashita and S. Kano, "Simulation Analysis of Geomagnetically Induced Currents (GIC) Effects on Shell-Form Transformers" Published in: Power and Energy Society General Meeting (PES), 2013 IEEE.
- [9] Kuan Zheng, David Boteler, Risto J. Pirjola, Lian-guang Liu, Richard Becker, Luis Marti, Stephen Boutilier, and Sebastien Guillon, "Effects of System Characteristics on Geomagnetically Induced Currents" IEEE Transaction on Power Delivery, Vol. 29, No. 2, April 2014.
- [10] D. H. Boteler and E. Bradley, "On the Interaction of Power Transformers and Geomagnetically Induced Currents" Published in: IEEE Transactions on Power Delivery, Pages: 2188 – 2195, Volume: 31, Issue: 5, Oct. 2016.

- [11] Afshin Rezaei-Zare, Luis Marti, Arun Narang and Andrew Yan, "Analysis of Three-Phase Transformer Response due to GIC using an Advanced Duality-Based Model" Published in: IEEE Transactions on Power Delivery, Pages: 2342 – 2350, Volume: 31, Issue: 5, Oct. 2016.
- [12] Waruna Chandrasena, Steve Shelemy, "A Review of Geomagnetic Disturbance (GMD) Effects in Manitoba" Published in: Power and Energy Society General Meeting (PES), 2013 IEEE. 1932-5517, Vancouver, BC, Canada, IEEE, 2013.
- [13] W. A. Radasky¹ and J. G. Kappenman, "Impacts of Geomagnetic Storms on EHV and UHV Power Grids" Asia-Pacific International Symposium on Electromagnetic Compatibility, April 12-16, 2010, Beijing, China.
- [14] Research Centre for Energy Networks - ETH Zurich, "Geomagnetically Induced Currents In The Swiss Transmission Network" Swiss Federal Office of Energy and swissgrid.
- [15] Lian-Guang Liu; Wei-Li Wu; Kuan Zheng, "Preliminary estimate of GIC risk in China's future power grid due to geomagnetic disturbance" 2013 IEEE Power & Energy Society General Meeting, Pages: 1-4, IEEE, 2013.
- [16] Thomas Halbedl; Herwig Renner; Rachel Louise Bailey; Roman Leonhardt; Georg Achleitner, "Analysis of the impact of geomagnetic disturbances on the Austrian transmission grid" 2016 Power Systems Computation Conference (PSCC), Year: 2016, Pages: 1-5, IEEE, 2016.
- [17] Matti Lahtinen, Member, IEEE, and Jarmo Elovaara, "GIC Occurrences and GIC Test for 400 kV System Transformer" IEEE Transactions On Power Delivery, Vol. 17, No. 2, April 2002.
- [18] Power & energy magazine IEEE, "Geomagnetic Disturbances, Their Impact on the Power Grid" Digital Object Identifier 10.1109/MPE.2013.2256651, IEEE, Date of publication: 19 June 2013.
- [19] Qun Qiu, Jeffery A. Fleeman, and David R. Ball, "Geomagnetic Disturbance, A comprehensive approach by American Electric Power to address the impacts" IEEE Electrification Magazine, Digital Object Identifier 10.1109/MELE.2015.2480615, IEEE, Date of publication: 2 December 2015.
- [20] Dr. Chris Beck, "The International E-Pro Report International Electric Grid Protection" Electric Infrastructure Security Council, Washington D.C., published September, 2013.

- [21] Luis Marti, "Introduction to GMD Studies, A Planner's Summary Roadmap for GMD Planning Studies Luis" NERC, December 9, 2015.
- [22] Sidwell Metetwa, "Specification For Power Transformers Rated For 1.25 MVA And Above And With Highest Voltage Of 2.2 kV Or Above" Escom Standard, Rev.0, 2014.
- [23] By S. Arabi and M. M. Komaragiri, "Effects of geomagnetically-induced currents in power transformers from power systems point of view" IEEE, Can. Elcc. Eng. J., Vol. 12 No. 4, 1987.
- [24] P. Picher, L. Bolduc, A. Dutil, V. Q. Pham, "Study Of The Acceptable Dc Current Limit In Core-Form Power Transformers" IEEE Transactions on Power Delivery, Vol. 12, No. 1, January 1997.
- [25] Jinxia Yao, Min Liu, Changyun Li, Qingmin Li, "Harmonics and Reactive Power of Power Transformers with DC Bias" Shandong Electric Power Research Institute, Shandong Electric Power Research Institute.
- [26] Christopher W. Harrison and Philip I. Anderson, "Characterization of Grain-Oriented Electrical Steels Under High DC Biased Conditions" IEEE Transactions On Magnetics, Vol. 52, No. 5, May 2016.
- [27] Baris Kovan and Francisco de León, "Mitigation of Geomagnetically Induced Currents by Neutral Switching" IEEE Transactions On Power Delivery, Vol. 30, No. 4, August 2015.
- [28] Zhuohong Pan, Xiaomao Wang, Bo Tan, Lin Zhu, Yong Liu, Yilu Liu and Xishan Wen, "Potential Compensation Method for Restraining the DC Bias of Transformers During HVDC Monopolar Operation" IEEE Transactions On Power Delivery, Vol. 31, No. 1, February 2016.
- [29] S.V. Kulkarni, S.A. Khaparde, "Transformer Engineering: Design and Practice" Second edition, 2004.
- [30] Grain oriented electrical steel card details of ThyssenKrupp steel supplier, Germany. www.thyssenkrupp-electrical-steel.com.
- [31] Crompton Greaves Belgium transformers manual, 2015.
- [32] The National Electrical Manufacturers Association (NEMA) published NEMA TR 1-2013 Transformers, Regulators and Reactors.
- [33] NERC Project 2013-03 GMD Mitigation, "Draft Benchmark Geomagnetic Disturbance Event," April 21, 2014.

- [34] Private correspondances with different electrical steel manufacturers.
- [35] Maryam Kazerooni, Hao Zhu, and Thomas J. Overbye, “Improved Modeling of Geomagnetically Induced Currents Utilizing Derivation Techniques for Substation Grounding Resistance” Ieee Transactions On Power Delivery, Vol. 32, No. 5, October 2017.
- [36] Maryam Kazerooni, Hao Zhu, Thomas J. Overbye, and David A. Wojtczak, “Transmission System Geomagnetically Induced Current Model Validation” IEEE Transactions On Power Systems, Vol. 32, No. 3, May 2017.
- [37] Vakhnina V.V., Kuvshinov A.A., Chernenko A.A., Kretov D.A., “Power Grid Configuration Influence on the Geomagnetically Induced Currents Value in Power Transformers” International Conference on Industrial Engineering, Applications and Manufacturing (ICIEAM), Togliatti, Russia, 2017.
- [38] Finite Element Method Magnetics Problem Manual in FEMM, Version 4.2, by David Meeker, October 2015.

Vitae

Name : AYYOUB WAEL AL HOURANI

Nationality : JORDANIAN

Date of Birth : 6/17/1987

Email : Ayyoub87@gmail.com

Address : Amman - Jordan

Academic Background : Bachelor Degree in Electrical Engineering from University of Jordan, Amman, Jordan 2010.
Master of Science in Electrical Engineering from King Fahd University of Petroleum and Minerals (KFUPM), Dhahran, Saudi Arabia, 2018.
Working at Saudi Power Transformers Company, Dammam, Saudi Arabia as a Senior Electrical Design Engineer of Power Transformers.